AWARD NUMBER: W81XWH-20-1-0353

TITLE: Polyploid Giant Cancer Cells Actuate Prostate Cancer Tumor Resistance and Lethal Phenotype

PRINCIPAL INVESTIGATOR: Sarah Amend

CONTRACTING ORGANIZATION: Johns Hopkins University, Baltimore, MD

REPORT DATE: July 2023

TYPE OF REPORT: Annual

PREPARED FOR: U.S. Army Medical Research and Development Command
Fort Detrick, Maryland 21702-5012

REPORT DOCUMENTATION PAGE

Form Approved
OMB No. 0704-0188

1. REPORT DATE	2. REPORT TYPE	3. DATES COVERED
July 2023	Annual	15Jun2022-14Jun2023

4. TITLE AND SUBTITLE

Polyploid Giant Cancer Cells Actuate Prostate Cancer Tumor Resistance and Lethal Phenotype

5a. CONTRACT NUMBER

5b. GRANT NUMBER
W81XWH-20-1-0353

5c. PROGRAM ELEMENT NUMBER

6. AUTHOR(S)
Sarah Amend

E-Mail: samend2@jhmi.edu

5d. PROJECT NUMBER

5e. TASK NUMBER

5f. WORK UNIT NUMBER

7. PERFORMING ORGANIZATION NAME(S) AND ADDRESS(ES)

Johns Hopkins University
600 N. Wolfe St.
Baltimore, MD 21287

University of Michigan
1105 N. University Ave, Ann Arbor, MI 48109

University of Maryland / Baltimore VA Medical Center
10 N. Greene Street, Baltimore, MD 21201-1524

8. PERFORMING ORGANIZATION REPORT NUMBER

9. SPONSORING / MONITORING AGENCY NAME(S) AND ADDRESS(ES)

U.S. Army Medical Research and Development Command
Fort Detrick, Maryland 21702-5012

10. SPONSOR/MONITOR'S ACRONYM(S)

11. SPONSOR/MONITOR'S REPORT NUMBER(S)

12. DISTRIBUTION / AVAILABILITY STATEMENT

Approved for Public Release; Distribution Unlimited

13. SUPPLEMENTARY NOTES

14. ABSTRACT

Lethal prostate cancer is incurable because the population of cancer cells within a tumor are resistant to all known compounds, including standard-of-care therapy. Resistance to a therapy may be solely cell intrinsic, therefore present in a treatment-naïve setting, as well as be induced through external selective pressure via therapeutic treatment. How and when drug resistance arises has profound implications to understand tumorigenesis as well as to guide treatment and management of disease. We and others have have demonstrated that the appearance of a subset of morphologically distinct cancer cells with high genomic content, polyploid giant cancer cells (PGCCs), is associated with therapeutic interventions. Based on our preliminary results, we hypothesize that PGCCs are central mediators of tumor resistance and prostate cancer lethality. To test this hypothesis, we will: 1) determine how and when PGCCs are formed during cancer progression and 2) demonstrate that quiescence underlies a common mechanism of stress resistance in PGCCs. The results of the above studies will fundamentally change our understanding of how and when therapeutic resistance arises during prostate tumorigenesis and its treatment course, specifically delineating the role of polyploid giant cancer cells as mediators of therapeutic resistance in prostate tumors. In the current term, we have begun to understand the mechanisms of PGCC formation resulting in a single nucleus or multiple nuclei. We have shown that PGCCs arise under multiple tumor microenvironmental stressors, including hypoxia and altered pH. We found that PGCCs under therapy exist in a G0 quiescent state. Finally, we have demonstrated that PGCCs have stem like properties, both in terms of function and molecular markers. This work has resulted in multiple peer-reviewed publications in the last year.

15. SUBJECT TERMS

Therapy resistance, polyploidy, polyaneuploid cancer cells, polyploid giant cancer cells, quiescence

16. SECURITY CLASSIFICATION OF:			17. LIMITATION OF ABSTRACT	18. NUMBER OF PAGES	19a. NAME OF RESPONSIBLE PERSON
a. REPORT	b. ABSTRACT	c. THIS PAGE			USAMRDC
Unclassified	Unclassified	Unclassified	Unclassified	35	19b. TELEPHONE NUMBER *(include area code)*

TABLE OF CONTENTS

1. **Introduction:**

Lethal prostate cancer is incurable because the population of cancer cells within a tumor are resistant to all known compounds, including standard-of-care therapy. Resistance to a therapy may be solely cell intrinsic, therefore present in a treatment-naïve setting, as well as be induced through external selective pressure via therapeutic treatment. How and when drug resistance arises has profound implications to understand tumorigenesis as well as to guide treatment and management of disease. We and others have have demonstrated that the appearance of a subset of morphologically distinct cancer cells with high genomic content, polyploid giant cancer cells (PGCCs), is associated with therapeutic interventions, including taxane-based chemotherapy in castrate resistant prostate cancer. The presence of PGCCs has been recognized for more than a century, but significance of these cells in tumor biology has been largely unexplored. Based on our preliminary results, we hypothesize that PGCCs mediate resistance and survive by existing in a dormant quiescent state and, upon a period of recovery, give rise to a resistant a resistant population of non-polyploid cells. Therefore, we hypothesize that PGCCs are central mediators of tumor resistance and prostate cancer lethality. To test this hypothesis, we will: 1) determine how and when PGCCs are formed during cancer progression and 2) demonstrate that quiescence underlies a common mechanism of stress resistance in PGCCs. The results of the above studies will fundamentally change our understanding of how and when therapeutic resistance arises during prostate tumorigenesis and its treatment course, specifically delineating the role of polyploid giant cancer cells as mediators of therapeutic resistance in prostate tumors.

1. Keywords:

Therapy resistance, polyploidy, polyaneuploid cancer cells, polyploid giant cancer cells, quiescence

2. Accomplishments

What were the major goals of the project?

Specific Aim 1. Determine how and when PGCCs are formed during prostate cancer progression
Major Task 1: Measure PGCCs in prostate cancer tissues in murine models.
Major Task 2: Measure PGCCs in patient TMAs

- Milestone #1: generate a novel prostate cancer progression TMA

Major Task 3: Determine the tumor microenvironment conditions to induce formation of PGCCs.
Major Task 4: Determine mechanism of PGCC formation

- Milestone #2: Submit manuscript on the role PGCCs in prostate cancer progression, including as a prognostic factor of disease progression/ response to therapy and how PGCCs are initially formed.

Specific Aim 2: Demonstrate that quiescence underlies a common mechanism of stress resistance in PGCCs
Major Task 1: Generate cell cycle reporter prostate cancer cell lines to be used in subsequent experiments

- Milestone #3: Develop and validate stable PC3 cell lines for prostate cancer research community that can be used to monitor quiescence entry/exit in vitro and in vivo.

Major Task 3: Examine quiescence markers in PGCCs under other treatment conditions that lead to resistance.
Major Task 4: Evaluate stem-cell properties of PGCCs.

- Milestone #4: Submit manuscript on entry and exit of quiescence and resistance in polyploid giant cancer cells in prostate cancer

What was accomplished under these goals?

Specific Aim 1. Determine how and when PGCCs are formed during prostate cancer progression
Major Task 1: Measure PGCCs in prostate cancer tissues in murine models.

- We have collected tumors and processed for IHC from all timepoints of GEMM model Hi-Myc. Initial QC of images has been completed. Scoring is currently underway.

- In addition, we are validating a semi-automated evaluation of polyploidy using StarDist (open access software) that will enable rapid and unbiased assessment of these samples.

Major Task 2: Measure PGCCs in patient TMAs

- The JHU prostate cancer progression TMA has been assessed. Our findings show that the number of PACCs and the number of cores positive for PACCs are statistically significant prognostic factors for metastasis-free survival, after adjusting for CAPRA-S, in a case-cohort of intermediate- or high-risk men who underwent radical prostatectomy. In addition, despite the small number of men with complete data to evaluate time to mCRPC, the total number of PACCs was a statistically significant predictor of mCRPC in univariate analysis, and suggested a prognostic effect even after adjusting for CAPRA-S.
- This data has been published: Trabzonlu L, Pienta KJ, Trock BJ, De Marzo AM, Amend SR. Presence of cells in the polyaneuploid cancer cell (PACC) state predicts the risk of recurrence in prostate cancer. Prostate. 2023 Feb;83(3):277-285. doi: 10.1002/pros.24459. Epub 2022 Nov 13. PMID: 36372998; PMCID: PMC9839595.
- We have generated the UM/BVMAC prostate tumor progression TMA (samples identified, cores taken, physical TMA built, slides cut, stained for H&E and IHC). We have also completed construction of a second TMA of this same patient source for metastatic lesions. Scoring of these TMAs is currently underway.

Major Task 3: Determine the tumor microenvironment conditions to induce formation of PGCCs.

- We showed in previous progress reports that PGCCs are generated upon exposure to hypoxia, altered pH, and overcrowding.
- We have shown that cells in the PACC state are resistant to subsequent challenge with other classes of cytotoxic chemotherapy, including docetaxel, cisplatin, and etoposide. This data is included in a recent publication (Kim CJ, Gonye AL, Truskowski K, Lee CF, Cho YK, Austin RH, Pienta KJ, Amend SR. Nuclear morphology predicts cell survival to cisplatin chemotherapy. Neoplasia. 2023 Aug;42:100906. doi: 10.1016/j.neo.2023.100906. Epub 2023 May 10. PMID: 37172462; PMCID: PMC10314150.)

Major Task 4: Determine mechanism of PGCC formation.

Our data indicate that cells under stress first pause in G2 at the G2/M cell cycle checkpoint. Cells then bypass the G2/M checkpoint, skip mitosis, and enter an endocycling cell state (repeated rounds of G- and S-phases in the absence of mitosis). We have reported that repeated rounds of whole genome doubling (WGD) results in very high polyploidy, at least to 16N. Confirming this data, we found that overall, surviving cells in the PACC state continue to increase in nuclear size and cell volume (to approx. 70x size).

Other work on WGD in the published literature suggests that stress, such as therapy, induces multinucleation. In contrast, our data indicate that a mononuclear phenotype predominates and becomes the majority phenotype in the days and weeks following therapy.

- This data formed the basis for a recent publication: Kim CJ, Gonye AL, Truskowski K, Lee CF, Cho YK, Austin RH, Pienta KJ, Amend SR. Nuclear morphology predicts cell survival to cisplatin chemotherapy. Neoplasia. 2023 Aug;42:100906. doi: 10.1016/j.neo.2023.100906. Epub 2023 May 10. PMID: 37172462; PMCID: PMC10314150.

Specific Aim 2: Demonstrate that quiescence underlies a common mechanism of stress resistance in PGCCs

Major Task 1: Generate cell cycle reporter prostate cancer cell lines to be used in subsequent experiments

As reported on previous progress reports, these cell lines have been engineered and confirmed and are in use.

Major Task 3: Examine quiescence markers in PGCCs under other treatment conditions that lead to resistance.

The specific FUCCI reported utilized was selected to distinguish all phases of the cell cycle, including G1, G2, and G0. As reported in the 2022 progress report, our data have disproven our hypothesis that PGCCs are quiescent. Instead, we find that cells in the PACC continue to endocycle and progress through G and S phases (versus cell cycle exit into G0). We have confirmed these data by life cell imaging, Ki67 stain, EdU incorporation, and Western Blot, and is further supported by the data described above.

In addition, we examined classical characteristics of senescence, and the data thus far suggests that PGCCs (cells in the PACC state) are likely accessing senescence programs. Pilot data indicate that cells in the PACC state do not divide (DiD dye retention), are B-gal positive, and the DAPI nuclear staining suggests presence of senescence-associated heterochromatin foci (SAHF). New preliminary data indicate that the cells express high levels of the Senescence Associated Secretory Phenotype (SASP), including IL6. Importantly, however, these cells are not classically senescent as they are actively engaged in cell cycle and will eventually undergo ploidy reduction (i.e., this is not a terminal state).

Major Task 4: Evaluate stem-cell properties of PGCCs.

We previously reported a "typical" parental cell morphology and ploidy population arises from PGCCs after a period of recovery. Preliminary single-cell RNAseq data indicate a heterogeneity of stem-like expression. Due to the heterogeneity and apparent temporal dependence of these expression profiles, we have turned our efforts to evaluating *functional* stem-like characteristics.

Efforts continue to "catch" ploidy reduction in time-lapse imaging. As this is a rare event, many hours of imaging of many replicates are required to record even a single event. Thus far, we have recorded symmetric cell division, but have been unable to track those progeny cells (they moved out of the field of view). A clear solution to this would be single-cell seeding into a multi-well plate to 1) verify a single PGCC is transferred and 2) permit depolyploidization and repopulation of the well. Since last year, we have overcome the practical challenges to this experiment. Specifically, we have increased initial seeding densities (seeding several 384w plates at a time), utilized a GFP-labeled cell line to improve imaging efficiency, and standardized imaging timelines. In addition, we have optimized the use of a WOLF G2 flow sorter that uses a fluidics-based system rather than a cuvette-based system for cell sorting.

Finally, we have altered hardware and downstream analysis on am Attune flow cytometer that, while it is not a cell sorter, enables high-throughput evaluation of single polyploid cells to confirm polyploid status of a population prior to seeding. This method development will be published in the coming 6 months.

Selected data included below.

See attached publications:

Kim CJ, Gonye AL, Truskowski K, Lee CF, Cho YK, Austin RH, Pienta KJ, Amend SR. Nuclear morphology predicts cell survival to cisplatin chemotherapy. Neoplasia. 2023 Aug;42:100906. doi: 10.1016/j.neo.2023.100906. Epub 2023 May 10. PMID: 37172462; PMCID: PMC10314150.

Trabzonlu L, Pienta KJ, Trock BJ, De Marzo AM, Amend SR. Presence of cells in the polyaneuploid cancer cell (PACC) state predicts the risk of recurrence in prostate cancer. Prostate. 2023 Feb;83(3):277-285. doi: 10.1002/pros.24459. Epub 2022 Nov 13. PMID: 36372998; PMCID: PMC9839595.

Selected data:

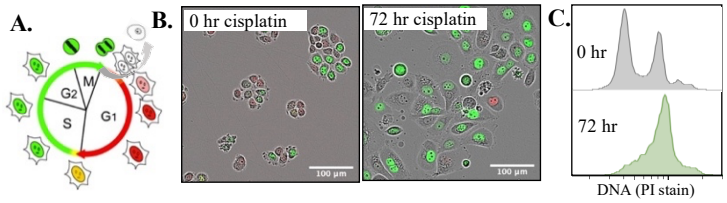

Surviving cells undergo initial G2 arrest. (A) Diagram of Ki67-FUCCI reporter. PC3-FUCCI cells were treated with 6 µm cisplatin for 72h **(B)** Live cell tracking shows nuclei are predominantly green, indicating G2 arrest (scale=100 µm). **(C)** Flow cytometry of DNA content (PI) confirms a majority G2 population.

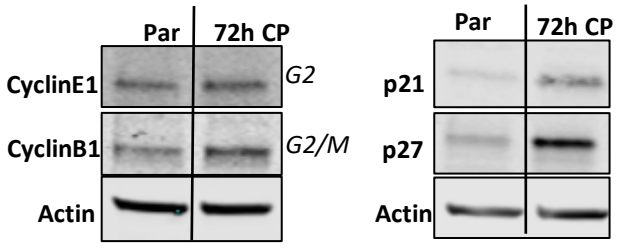

Western blot markers are consistent with a G2/M arrest after 72h treatment. Cyclin E1 is expressed in G2 and Cycling B1 is expressed at the G2/M boundary. Both are present (and perhaps enriched – further replicates are required) following treatment. Cell cycle inhibitors p21 and p27 are both induced following 72h treatment, indicating that cell cycle progression is inhibited.

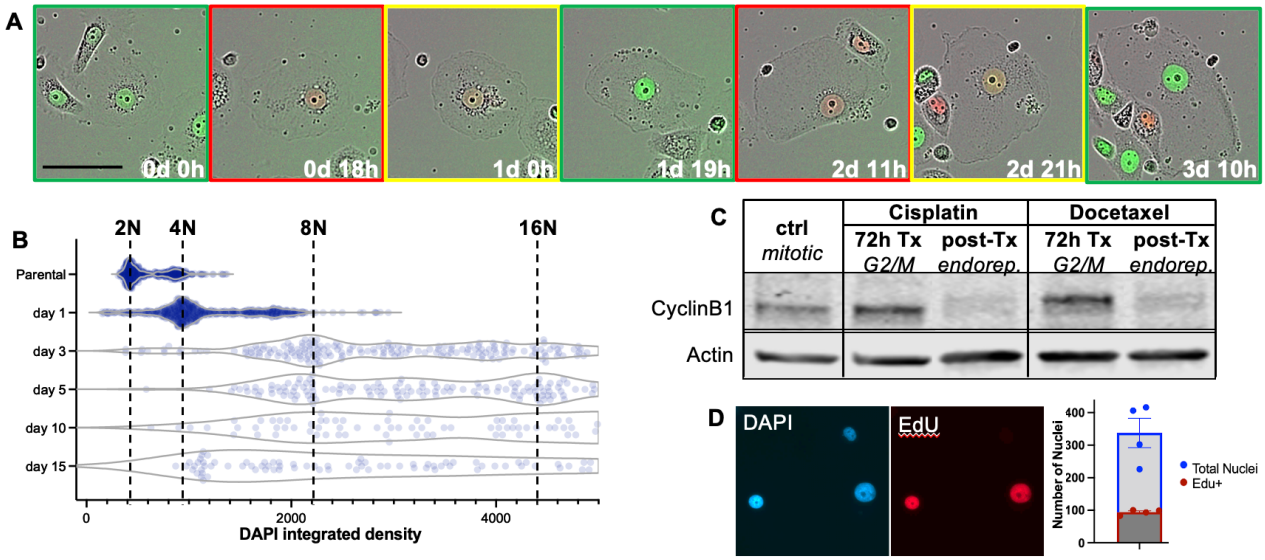

Fig 4. Cells that survive after therapy enter an endoreplicative cell cycle and undergo WGD.
(A) PC3-FUCCI cells were treated with LD50 cisplatin for 72h. After drug was washed out, cells were monitored by live cell fluorescent imaging. Still images from movie following a single cell that endoreplicates multiple times over 3 days without entering mitosis (red = G1; yellow = early S; green = G2). scale bar = 100 µm; (B) Integrated density of DAPI signal as a measure of DNA content. Dotted lines indicate relative ploidy based on G1/G2M cell cell cycle of the proliferative parental population. (Cisplatin treated PC3; days indicate release from treatment; from imaging of DAPI-stained cells); **(C)** PC3 cells were treated with LD50 cisplatin or docetaxel for 72h and drug was washed out. Immediately after treatment (72h), CyclinB (elevated at G2/M) is elevated; CyclinB is absent in cells that survive 10 (cisplatin) or 5 days (docetaxel) post-treatment. **(D)** surviving and non-dividing PC3 cells (10 days post-72h LD50 cisplatin treatment) were labeled with EdU (20 hr). ~20% of DAPI+ nuclei were EdU+.

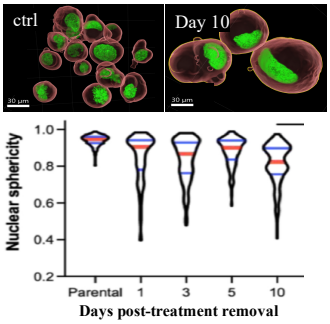

Therapy-induced endoreplicative cells have hallmarks of an endocycling mechanism. PC3 cells were treated with 72h LD50 cisplatin and treatment released for 10 days. Nuclear sphericity was measured from confocal images of LaminA/C nuclear envelope stain. (scale bar 30 µm Perfect sphere=1.0)

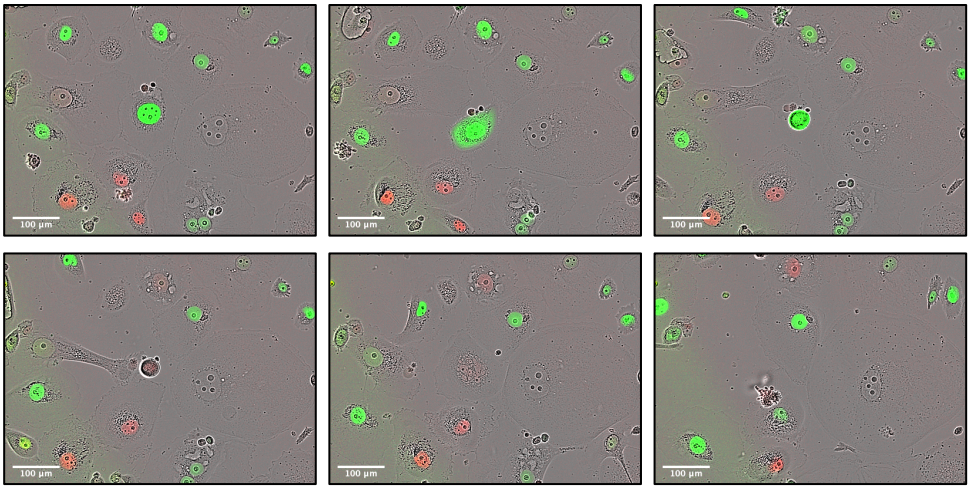

Cycling polyploid cells that enter mitosis undergo apoptosis. Using single-cell tracking of FUCCI reporters, we find that endocycling polyploid cells that prematurely enter mitosis (i.e., prior to ploidy reduction) undergo mitosis. These still images are tracking a single polyploid cell over time. Breakdown of the nuclear envelope is evident in frame 2; mitotic rounding in frame 3-4; cell apoptosis debris is appreciable in frame 6.

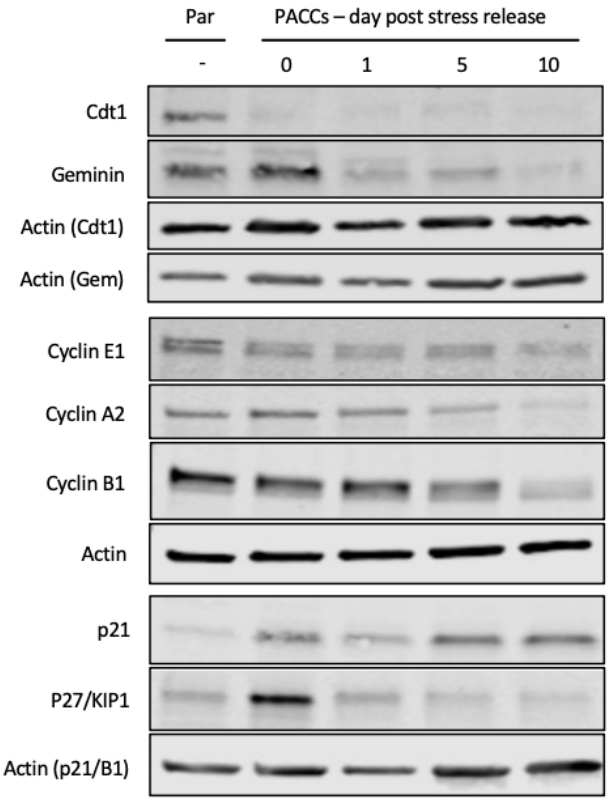

Western blots of cell cycle markers: PC3 prostate cancer cells were cultured under stress (shown for cisplatin) for 72h and released for 0, 1, 5, or 10 days. Untreated parental served as control
Immunoblot for Cdt1 (active in G1/early S), Geminin (active in S/G2/M), Cyclin E1 (G1/S), Cyclin A2 (G2), Cyclin B1 (M), and cell cycle inhibitors p21 and p27 (classical markers of G0-quiescence).

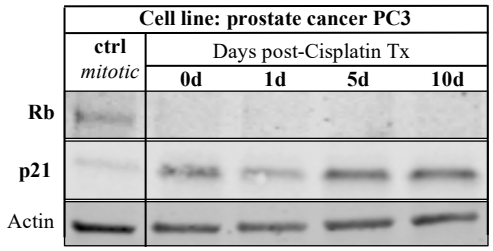

Therapy-induced polyploid cells are Rb-low and p21-high. (Rb and p21 are essential regulators of the cell cycle through G1/S and G2 – this work was done to understand progression during polyploidization). Cell lysates were collected from untreated mitotic cells and endoreplicative PC3 cells days 72h LD50 cisplatin treatment. Rapid loss of Rb and sustained p21 expression is reproducibly observed across cell lines.

What opportunities for training and professional development has the project provided?
Nothing to report.

How were the results disseminated to communities of interest?

Results were presented to the scientific community in the form of manuscripts and presentations (listed below).

What do you plan to do during the next reporting period to accomplish the goals?
Over the next reporting period, we aim to 1) complete TMA and GEMM analysis and 2) continue the described *in vitro* studies as outlined in the SOW. With all positions once again filled, we anticipate the proposed research to advance as projected.

4. Impact

What was the impact on the development of the principal discipline(s) of the project?
This work has contributed to the understanding of therapy resistance in cancer – in prostate cancer specifically as well as other solid tumors. In addition, with the data indicating that PGCC index (now named PACC index) has prognostic value, there is a likelihood of impacting clinical care of prostate cancer patients.

What was the impact on other disciplines?

This work has informed the understanding of evolution of resistant cancer cells across multiple tumor types, including informing collaborations with other groups studying breast cancer and lung cancer.

What was the impact on technology transfer?
Nothing to report in from the last year.

What was the impact on society beyond science and technology?
Nothing to report.

5. Changes/Problems

Changes in approach and reasons for change
No major changes in approach have been made or are planned.
Minor changes in approach:

1. Due to challenges with animal colonies, we will reply upon the GEMM Hi-Myc for the animal studies.

Actual or anticipated problems or delays and actions or plans to resolve them
We have encountered related major delays that have unexpectedly slowed progress:

1) RESOLVED: As previously reported: COVID-19-related delays: The research labs at Johns Hopkins were closed from March 18, 2020 – June 15, 2020. Though this pre-dated this grant period, this resulted in unavoidable delays related to this work that is extending into the current period. Specifically, during this lab shutdown, animal colonies – including the TRAMP and hi-Myc colonies to be used in the proposed work – had to be scaled back dramatically, only including breeders necessary for maintaining the lines. It has taken several months to recover these colonies to the point where selection and aging of animals can begin. During this process and due to understaffing, the TRAMP colony breeding was discontinued in order to maintain a robust hi-MYC colony. The Hi-Myc colony is now re-established and we are awaiting the 12 month cohort.
2) RESOLVED AND ONGOING As previously reported: Hiring delays: The lab technologist originally listed in the proposal left for another position in early January 2020. Hiring delays prevented immediate backfilling of this position. The position was filled as of June 1, 2021, but the lab technologist resigned in July 2021. This position has now been re-posted and filled, as of June 2022. This individual held the role for approx. 6 months and then took on a different and higher-level role. It was back-filled again as of January 2023. Due to the applicant pool for the position, these newly hired staff member have had substantially less research experience anticipated, with resulting lower productivity. I anticipate that, after a period of training for basic laboratory skills, their productivity to increase. In addition, since this grant was submitted, the PI's lab has expanded in size, and some of the proposed research has been undertaken by Ph.D. students and a postdoctoral fellow.

Changes that had a significant impact on expenditures
Nothing to report beyond previous reports (that led to a request for NCE).

Significant changes in use or care of human subjects, vertebrate animals, biohazards, and/or select agents
Nothing to report.

Significant changes in use or care of human subjects
Nothing to report.

Significant changes in use or care of vertebrate animals.
Nothing to report.

Significant changes in use of biohazards and/or select agents.
Nothing to report.

6. Products

Journal publications

Cancer cells employ an evolutionarily conserved polyploidization program to resist therapy. Pienta KJ, Hammarlund EU, Austin RH, Axelrod R, Brown JS, Amend SR. Semin Cancer Biol. 2022 Jun;81:145-159. doi: 10.1016/j.semcancer.2020.11.016. Epub 2020 Dec 1. Published, acknowledgement of federal support.

Cancer cell foraging to explain bone-specific metastatic progression. Mallin MM, Pienta KJ, Amend SR. Bone. 2022 May;158:115788. doi: 10.1016/j.bone.2020.115788. Epub 2020 Dec 3. Published, acknowledgement of federal support.

Extracellular Vesicle Uptake Assay via Confocal Microscope Imaging Analysis. Kim CJ, Kuczler MD, Dong L, Kim J, Amend SR, Cho YK, Pienta KJ. J Vis Exp. 2022 Feb 14;(180). doi: 10.3791/62836. Published, acknowledgement of federal support.

Advancements in the identification of EV derived mRNA biomarkers for liquid biopsy of clear cell renal cell carcinomas. Kuczler MD, Zieren RC, Dong L, de Reijke TM, Pienta KJ, Amend SR. Urology. 2022 Feb;160:87-93. doi: 10.1016/j.urology.2021.11.002. Epub 2021 Nov 15. Published, acknowledgement of federal support.

ROS-induced cell cycle arrest as a mechanism of resistance in polyaneuploid cancer cells (PACCs). Kuczler MD, Olseen AM, Pienta KJ, Amend SR. Prog Biophys Mol Biol. 2021 Oct;165:3-7. doi: 10.1016/j.pbiomolbio.2021.05.002. Epub 2021 May 12. Published, acknowledgement of federal support.

Lipid droplet evolution gives insight into polyaneuploid cancer cell lipid droplet functions. Kostecka LG, Pienta KJ, Amend SR. Med Oncol. 2021 Sep 28;38(11):133. doi: 10.1007/s12032-021-01584-w. Published, acknowledgement of federal support.

The role of liquid biopsies in prostate cancer management. Kim CJ, Dong L, Amend SR, Cho YK, Pienta KJ. Lab Chip. 2021 Sep 7;21(17):3263-3288. doi: 10.1039/d1lc00485a. Epub 2021 Aug 4. Published, acknowledgement of federal support.

Twelve unanswered questions in cancer inspired by the life and work of Leland Chung: "if this is true, what does it imply"? Li M, Gonye AL, Truskowski K, Loftus LV, Urbanski LA, Myers KV, Mallin MM, Yang ME, Mendez SA, Kostecka LG, Udedibor CR, Kim CJ, Kuczler MD, Shin GH, Amend SR, Pienta KJ. Am J Clin Exp Urol. 2021 Aug 25;9(4):254-260. eCollection 2021. Published, acknowledgement of federal support.

Defining candidate mRNA and protein EV biomarkers to discriminate ccRCC and pRCC from non-malignant renal cells in vitro. Zieren RC, Dong L, Clark DJ, Kuczler MD, Horie K, Moreno LF, Lih TM, Schnaubelt M, Vermeulen L, Zhang H, de Reijke TM, Pienta KJ, Amend SR. Med Oncol. 2021 Jul 31;38(9):105. doi: 10.1007/s12032-021-01554-2. Published, acknowledgement of federal support.

Characterization of tumor-associated macrophages in prostate cancer transgenic mouse models. de Groot AE, Myers KV, Krueger TEG, Kiemen AL, Nagy NH, Brame A, Torres VE, Zhang Z, Trabzonlu L, Brennen WN, Wirtz D, De Marzo AM, Amend SR, Pienta KJ. Prostate. 2021 Jul;81(10):629-647. doi: 10.1002/pros.24139. Epub 2021 May 5. Published, acknowledgement of federal support.

Wang G, Phan TV, Li S, Wang J, Peng Y, Chen G, Qu J, Goldman DI, Levin SA, Pienta K, Amend S, Austin RH, Liu L. Robots as models of evolving systems. Proc Natl Acad Sci U S A. 2022 Mar 22;119(12):e2120019119. doi: 10.1073/pnas.2120019119. Epub 2022 Mar 17.

Wang Y, Lih TM, Chen L, Xu Y, Kuczler MD, Cao L, Pienta KJ, Amend SR, Zhang H. Optimized data-independent acquisition approach for proteomic analysis at single-cell level. Clin Proteomics. 2022 Jul 9;19(1):24. doi: 10.1186/s12014-022-09359-9.

Bukkuri A, Pienta KJ, Austin RH, Hammarlund EU, Amend SR, Brown JS. Stochastic models of Mendelian and reverse transcriptional inheritance in state-structured cancer populations. Sci Rep. 2022 Jul 29;12(1):13079. doi: 10.1038/s41598-022-17456-w.

Bukkuri A, Pienta KJ, Austin RH, Hammarlund EU, Amend SR, Brown JS. A life history model of the ecological and evolutionary dynamics of polyaneuploid cancer cells. Sci Rep. 2022 Aug 12;12(1):13713. doi: 10.1038/s41598-022-18137-4.

de Groot AE, Myers KV, Krueger TEG, Brennen WN, Amend SR, Pienta KJ. Targeting interleukin 4 receptor alpha on tumor-associated macrophages reduces the pro-tumor macrophage phenotype. Neoplasia. 2022 Oct;32:100830. doi: 10.1016/j.neo.2022.100830.

Dong L, Du X, Lu C, Zhang Z, Huang CY, Yang L, Warren S, Kuczler MD, Reyes DK, Luo J, Amend SR, Xue W, Pienta KJ. RNA profiling of circulating tumor cells systemically captured from diagnostic leukapheresis products in prostate cancer patients. Mater Today Bio. 2022 Dec 15;17:100474. doi: 10.1016/j.mtbio.2022.100474.

Trabzonlu L, Pienta KJ, Trock BJ, De Marzo AM, Amend SR. Presence of cells in the polyaneuploid cancer cell (PACC) state predicts the risk of recurrence in prostate cancer. Prostate. 2023 Feb;83(3):277-285. doi: 10.1002/pros.24459. Epub 2022 Nov 13

Bukkuri A, Pienta KJ, Hockett I, Austin RH, Hammarlund EU, Amend SR, Brown JS. Modeling cancer's ecological and evolutionary dynamics. Med Oncol. 2023 Feb 28;40(4):109. doi: 10.1007/s12032-023-01968-0.

Truskowski K, Amend SR, Pienta KJ. Dormant cancer cells: programmed quiescence, senescence, or both?. Cancer Metastasis Rev. 2023 Mar;42(1):37-47. doi: 10.1007/s10555-022-10073-z.

Haney NM, Kim CJ, Kuczler MD, Lee CF, Lombardo K, Bivalacqua TJ, Pienta KJ, Amend SR. Novel urinary tract obstruction marker discovery by multi-marker profiling of urinary extracellular vesicles derived from a rat UTO model. Am J Clin Exp Urol. 2023;11(2):136-145

Mallin MM, Kim N, Choudhury MI, Lee SJ, An SS, Sun SX, Konstantopoulos K, Pienta KJ, Amend SR. Cells in the polyaneuploid cancer cell (PACC) state have increased metastatic potential. Clin Exp Metastasis. 2023 Aug;40(4):321-338. doi: 10.1007/s10585-023-10216-8. Epub 2023 Jun 16.

Kim CJ, Gonye AL, Truskowski K, Lee CF, Cho YK, Austin RH, Pienta KJ, Amend SR. Nuclear morphology predicts cell survival to cisplatin chemotherapy. Neoplasia. 2023 Aug;42:100906. doi: 10.1016/j.neo.2023.100906. Epub 2023 May 10.

Other publications, conference papers, and presentations.

Invited presentations:

Prostate SPORE meeting (monthly national meeting of all Prostate SPORE teams), NIH/NCI, “The polyaneuploid transition (PAT) actuates therapy resistance and cancer lethality”; Multiple locations (virtual via WebEx)

NIH Liquid biopsy scientific interest group (SIG), NIH/NCI, “Extracellular vesicles (EVs) as a source of liquid biopsy biomarkers in urological cancer”; Bethesda, MD (virtual via WebEx)

14th Annual Prostate Cancer Program Retreat of the NCI Prostate SPOREs, “Engaging the polyaneuploid transition: a novel route to therapy resistance, dormancy, and metastasis”; Los Angeles, CA

Convergent Science Institute in Cancer, USC Michelson Center, University of Southern California, “Exploring the polyaneuploid cancer cell state to treat resistant cancer”; Los Angeles, CA

First Cell Summit, Columbia University, “The polyaneuploid cancer (PACC) in lethal cancer,” New York, NY

Cancer, Multicellularity and Complex Systems (A Royal Physiographic Society Jubilee Symposium), “The cancer ecology of lethal cancer;” Lund, Sweden

American Association for Cancer Research (AACR) Cancer Evolution Working Group (CEWG) Seminar Series, “Optimal Foraging Theory to Understand the Adaptive Strategies that Drive Lethal Cancer”

Cancer and Bone Society Conference, “Beyond seed and soil: the adaptive strategies that drive lethal cancer;” St. Louis, MO

Abstracts presented at national meetings:

Bukkuri, Anuraag, et al. "Abstract B015: Eco-evolutionary dynamics of poly-aneuploid cancer cells: A life history model." *Cancer Research* 82.10_Supplement (2022): B015-B015.

Bukkuri, Anuraag, et al. "Abstract A001: Modeling cancer’s ecological and evolutionary dynamics." *Cancer Research* 82.10_Supplement (2022): A001-A001.

Carroll, Christopher P., et al. "Abstract B018: Targeting Notch4 and HIF2α signaling reduces the ability of cells to survive chemotherapy by undergoing the polyaneuploid transition." *Cancer Research* 82.10_Supplement (2022): B018-B018.

Butler, George, et al. "Abstract B022: The polyaneuploid transition as a hedge against failures in resistance acquisition." *Cancer Research* 82.10_Supplement (2022): B022-B022.

Myers, Kayla V., et al. "Targeting MerTK-mediated efferocytosis in the prostate cancer TME." *Cancer Research*82.12_Supplement (2022): 2546-2546.

Gonye, Anna, et al. "Polyaneuploid prostate cancer cells induced via chemotherapy have predominantly large, single nuclei." *Cancer Research* 82.12_Supplement (2022): 140-140.

Kostecka, Laurie Gayle, Sarah Amend, and Kenneth Pienta. "The poly-aneuploid cancer cell state utilizes lipid droplets as a mechanism of survival." *Cancer Research* 82.12_Supplement (2022): 3017-3017.

Kuczler, Morgan D., Kenneth J. Pienta, and Sarah R. Amend. "Reactive oxygen species (ROS) as mediators of the cancer cell’s transition into the polyaneuploid cancer cell (PACC) state." *Cancer Research* 82.12_Supplement (2022): 123-123.

Li, Melvin, Sarah R. Amend, and Kenneth J. Pienta. "The role of oxidative stress on the polyaneuploid cancer cell state in metastatic cancer." *Cancer Research* 82.12_Supplement (2022): 125-125.

A Gonye, CJ Kim, K Pienta, S Amend, “Investigating the epigenetic landscape of chemotherapy-induced polyaneuploid prostate cancer cells,” Cancer Research 82 (23_Supplement_2), A028-A028

R Austin, K Shen, N Hosny, K Pienta, S Amend, E Hammarlund, "The effects of hypoxia on cancer cell motility and on cell size," Bulletin of the American Physical Society, 2023

R Austin, J Bos, G Butler, K Pienta, S Amend, "Heterogeneity in bacterial filamentation survival dynamics decrease in response to increased stress," Bulletin of the American Physical Society

C Lee, M Loycano, L Loftus, L Kostecka, M Li, S Amend, K Pienta, "A non-canonical CDK9 complex mediates endocycling in polyaneuploid cancer cell (PACC) state," Cancer Research 83 (7_Supplement), 5988-5988

SA Mendez, R Sharma, KJ Pienta, SR Amend, KRTAP 2-3 is a novel potential biomarker of cells in the polyaneuploid cancer cell (PACC) state to predict cancer recurrence, Cancer Research 83 (7_Supplement), 2205-2205

LG Kostecka, A Le, S Amend, KJ Pienta, Polyaneuploid cancer cells are metabolically active and utilize lipid droplets to survive toxic stress, Cancer Research 83 (7_Supplement), 6055-6055

M Loycano, KJ Pienta, SR Amend, Myc suppression permits entry into the cancer endocycle to evade toxic effects of chemotherapy, Cancer Research 83 (7_Supplement), 1690-1690

M Li, LG Kostecka, SR Amend, KJ Pienta, Stress-induced mitochondrial adaptations in the polyaneuploid cancer cell state, Cancer Research 83 (7_Supplement), 4842-4842

Mikaela M Mallin, Nicholas Kim, Mohammad Ikbal Choudhury, SeJong Lee, Steven S An, Sean X Sun, Konstantinos Konstantopoulos, Sarah R Amend, Kenneth J Pienta, "Polyaneuploid Cancer Cells (PACCs) as metastasis-competent cells," Cancer Research 83 (2_Supplement_2), A017-A017

Robert Austin, Yusha Sun, David Liao, Gonzalo Torga, Trung Phan, Joel Brown, Emma Hammarlund, Sarah Amend, Kenneth Pienta, "The physics of cancer recurrence and metastasis," Bulletin of the American Physical Society, 2023

Robert Austin, Kenneth Pienta, Chi-Ju Kim, Anna Gonye, Kevin Truskowski, Cheng-Fan Lee, Yoon-Kyoung Cho, Sarah Amend, Impact of the cancer endocycle on cell survival after therapy, Bulletin of the American Physical Society, 2023

Inventions, patent applications, and/or licenses
Provisional patent was registered related in part to the findings of PGCC index on patient TMAs (A Method to Diagnose, Predict Prognosis, and Treat Cancer by Identifying Cells in the Polyaneuploid Cancer Cell state). Provisional application files on June 3, 2022.

Other products
Two TMAs (tissue microarray) was completed from the UM radical prostatectomy specimens as outlined above.

7. Participants & other collaborating organizations

What individuals have worked on the project?
Sarah Amend no change

Name:	Chi-Ju Kim
Project Role:	Postdoctoral fellow
Researcher Identifier (e.g., ORCID ID)	
Nearest person month worked:	5
Contribution to project:	Dr. Kim is co-advised by Dr. Amend and has completed work related to nuclear structure and ploidy of cells in the PACC state / PGCCs.
Funding Support:	Dr. Kim is supported by a Nurturing Next-Generation Researchers Overseas Fellowship from the National Research Foundation (NRF), Korea

Name:	Kevin Truskowski
Project Role:	Graduate student
Researcher Identifier (e.g., ORCID ID)	
Nearest person month worked:	6
Contribution to project:	Mr. Truskowski is a graduate student co-advised by Dr. Amend. He completed the quiescence and senescence studies.
Funding Support:	Mr. Truskowski was supported by this grant and departmental support from the Dept of Urology.

Name:	**Shilpa Priyadarsini Nair**
Project Role:	Research Technologist /Specialist
Researcher Identifier (e.g., ORCID ID)	
Nearest person month worked:	3
Contribution to project:	Ms. Nair is a research tech (now specialist) in the Amend laboratory. She provided technical support, including cell culture, imaging, etc., of these studies.
Funding Support:	Ms. Gonye was supported by this grant.

Name:	Anna Gonye
Project Role:	Graduate student
Researcher Identifier (e.g., ORCID ID)	
Nearest person month worked:	6
Contribution to project:	Ms. Gonye is a graduate student in the Amend lab. She completed work related to nuclear structure, time lapse imaging, and work related to stemness and depolyploidization.
Funding Support:	Ms. Gonye was supported by her PhD program (Cellular and Molecular Medicine) and departmental support from the Dept of Urology.

Name:	Jing, Yuezhou
Project Role:	Technologist (Dept of Pathology)
Researcher Identifier (e.g., ORCID ID)	
Nearest person month worked:	2
Contribution to project:	Ms. Jing works in the De Marzo laboratory. She completed work related to sectioning, staining, QC of IHC/H&E images, and evaluation of markers/automated analysis.
Funding Support:	Ms. Jing was supported by this grant for the related work

Has there been a change in the active other support of the PD/PI(s) or senior/key personnel since the last reporting period?

DeMarzo: Updates are below:

W81XWH-22-1-0680 (Amend)
Title: PC210350 - The polyaneuploid cancer cell state mediates multi-therapy resistance in cancer
Effort: 0.43 calendar (3.63%)
Supporting Agency: CDMRP
Address of Funding Agency: 820 Chandler St., Fort Detrick, MD 21702-5014
Performance Period: 08/15/2022-08/14/2025
Level of Funding:
Project's Goal/Specific Aims: The primary goal of this study is to test the hypothesis that PACCs facilitate therapeutic resistance, and unless they are eradicated, cancer will recur in treated prostate cancer patients.
Projects overlap or parallel: No scientific or budgetary overlap

U54CA274370 (De Marzo/Yegnasubramanian)
Title: Prostate inflammatory lesions as a proving ground for development of aggressive prostate cancer
Effort: 1.78 calendar months (11.44%); [Admin Core: 3.71%, Project 1: 7.43%, Biopath Core: 3.71%]
Supporting Agency: NCI
Address of Supporting Agency: 6116 Executive Boulevard, Suite 7013, MSC 8347, Rockville, MD 20852
Performance Period: 09/15/2022-08/31/2027
Level of Funding:
Project Goal: To characterize the influence of tumor cells on disease progression in mice with combined MYC activation and PTEN loss.
Aim 1: To test the STING activation hypothesis for developing acute and chronic inflammation, PIA and PIN in the mouse prostate.
Aim 2: Comprehensive characterization of genomic and epigenomic changes in mouse and human epithelial cells in the transitions from prostatic inflammatory lesions to neoplasia.
Aim 3: Defining the cellular composition and spatial architecture of immune and stromal compartments of the TME in mouse and human precursor prostatic inflammatory lesions.
Overlap: No scientific or budgetary overlap.

90102524 (De Marzo)
Title: GAP1 Unique TMA Biorepository (MGTB) and Collaborative Agreement
Effort: 0.60 calendar (5%)
Supporting Agency: Movember Foundation
Address of Funding Agency: Culver City, CA 90232
Performance Period: 11/10/2022-12/31/2025
Level of Funding:
Project's Goal/Specific Aims: The aim of the project is to develop a TMA resource that can be used by the GAP1 investigators and the wider research community.
Projects overlap or parallel: No scientific or budgetary overlap

1317000027 (De Marzo)
Title: Testing the Proving Ground Hypothesis in Prostate Cancer **Effort:** 0.18 calendar months (1.49%)
Supporting Agency: Allegheny Health Network
Performance Period: 04/01/22-03/31/24
Level of Funding:
Project Goal: We hypothesize that chronic inflammation is a key driver of many early prostate cancers. Further, the inflammatory signals in the epithelial cells must be abrogated in order for the cancer to progress.
Overlap: No scientific or budgetary overlap.

HT94252310390 (Shenderov)
Title: PC220558 Utilizing B7-H3 Targeted Therapeutics to Prevent Lethal Prostate Cancer: The Help Elucidate & Attack Longitudinally (HEAL) Prostate Cancer Trial Cohort

Effort: 0.60 calendar months (5%)
Supporting Agency: CDMRP
Performance Period: 07/2023-06/2026
Level of Funding:
Project Goal: The primary clinical objective of this study is to properly power and investigate whether inhibition of B7-H3 via administration of enoblituzumab delays or prevents recurrence following prostatectomy compared to standard of care (SOC).
Aim 1: To examine pathologic and adaptive immunologic effects, and whether neoadjuvant B7-H3-directed treatment enhances the systemic priming of antitumor T-cells to eliminate micrometastatic disease responsible for postsurgical relapse.
Aim 2: To determine mechanisms of response and resistance to B7-H3 targeted immunotherapy at the time of lethal prostate cancer diagnosis through comprehensive disease imaging features (conventional imaging and PSMA), genomic DNA and spatial tumor microenvironment [TME] RNA dynamics),
metabolomics, as well as proteomic (serum and TME) signature of responders versus non-responders to enoblituzumab in both European- and African-ancestry patient.
Aim 3: To elucidate the B7-H3 receptor and describe intratumoral B7-H3 signaling to develop new B7-H3 targeted agents including B7-H3 ligand-receptor blockers and cell intrinsic blockers to prevent pro-proliferative signaling.
Overlap: No scientific or budgetary overlap.

Amend: updates are below:

W81XWH2210680
Title: PC210350 – The Polyaneuploid Cancer Cells State Mediates Multi-Therapy resistance in Cancer **Time Commitment:** 3.6 calendar months
Supporting Agency: CDMRP (PI – Amend)
Name of Procuring Contracting/Grants Officer: Ashley Evans
Address of Agency: 820 Chandler Street, Fort Dietrick MD 21702-5014
Performance Period: 08/15/2022 – 08/14/2025
Level of Funding:
Project Goal: The primary goal of this study is to test the hypothesis that PACCs facilitate therapeutic resistance, and unless they are eradicated, cancer will recur in treated prostate cancer patients.
Specific Aims:
1: Map the life history of the therapy-induced polyaneuploid transition.
2: Targeting the polyaneuploid transition state to overcome therapy resistance.
Role: PI
Project overlap or parallel: There is no scientific or budgetary overlap.

What other organizations were involved as partners?

Nothing to report.

8. Special reporting requirements

N/A

9. Appendices

2 published manuscripts in the reporting period directly related to this project.

Received: 14 April 2022 | Accepted: 1 November 2022

DOI: 10.1002/pros.24459

ORIGINAL ARTICLE

The Prostate WILEY

Presence of cells in the polyaneuploid cancer cell (PACC) state predicts the risk of recurrence in prostate cancer

Levent Trabzonlu MD[1] | Kenneth J. Pienta MD[2] | Bruce J. Trock PhD[3] | Angelo M. De Marzo MD, PhD[4] | Sarah R. Amend PhD[2]

[1]Department of Pathology and Laboratory Medicine, Loyola University Medical Center, Maywood, Illinois, USA

[2]Cancer Ecology Center, The Brady Urological Institute, Johns Hopkins University School of Medicine, Baltimore, Maryland, USA

[3]The Brady Urological Institute, Johns Hopkins School of Medicine, Baltimore, Maryland, USA

[4]Departments of Pathology, Urology and Oncology, The Johns Hopkins University School of Medicine, The Sidney Kimmel Comprehensive Cancer Center at Johns Hopkins, Baltimore, Maryland, USA

Correspondence

Sarah R. Amend, PhD, Cancer Ecology Center, The Brady Urological Institute, Johns Hopkins University School of Medicine, Baltimore, MD, USA.
Email: samend2@jhmi.edu

Funding information

Prostate Cancer Foundation; National Cancer Institute, Grant/Award Numbers: CA006973, CA093900, CA143055, CA163124, CA1936390, P50CA058236, P50CA58236, U54CA143803; Congressionally Directed Medical Research Programs, Grant/Award Numbers: W81XWH-18-2-0015, W81XWH-20-10353, W81XWH-21-0-373; Patrick C. Walsh Prostate Cancer Research Fund

Abstract

Background: The nonproliferating polyaneuploid cancer cell (PACC) state is associated with therapeutic resistance in cancer. A subset of cancer cells enters the PACC state by polyploidization and acts as cancer stem cells by undergoing depolyploidization and repopulating the tumor cell population after the therapeutic stress is relieved. Our aim was to systematically assess the presence and importance of this entity in men who underwent radical prostatectomy with curative intent to treat their presumed localized prostate cancer (PCa).

Materials and Methods: Men with National Comprehensive Cancer Network intermediate- or high-risk PCa who underwent radical prostatectomy I from 2007 to 2015 and who did not receive neoadjuvant treatment were included. From the cohort of 2159 patients, the analysis focused on a subcohort of 209 patients and 38 cases. Prostate tissue microarrays (TMAs) were prepared from formalin-fixed, paraffin-embedded blocks of the radical prostatectomy specimens. A total of 2807 tissue samples of matched normal/benign and cancer were arrayed in nine TMA blocks. The presence of PACCs and the number of PACCs on each core were noted.

Results: The total number of cells in the PACC state and the total number of cores with PACCs were significantly correlated with increasing Gleason score ($p = 0.0004$) and increasing Cancer of the Prostate Risk Assessment Postsurgical (CAPRA-S) ($p = 0.004$), but no other variables. In univariate proportional hazards models of metastasis-free survival, year of surgery, Gleason score (9–10 vs. 7–8), pathology stage, CAPRA-S, total PACCs, and cores positive for PACCs were all statistically significant. The multivariable models with PACCs that gave the best fit included CAPRA-S. Adding either total PACCs or cores positive for PACCs to CAPRA-S both significantly improved model fit compared to CAPRA-S alone.

Conclusion: Our findings show that the number of PACCs and the number of cores positive for PACCs are statistically significant prognostic factors for metastasis-free survival, after adjusting for CAPRA-S, in a case–cohort of intermediate- or high-risk men who underwent radical prostatectomy. In addition, despite the small number of

men with complete data to evaluate time to metastatic castration-resistant PCa (mCRPC), the total number of PACCs was a statistically significant predictor of mCRPC in univariate analysis and suggested a prognostic effect even after adjusting for CAPRA-S.

KEYWORDS
PACC, PGCC, polyaneuploid cancer cell, polyploid giant cancer cell, prostate cancer

1 | INTRODUCTION

Therapeutic resistance in cancer is generally attributed to the existence of resistant cell clones.[1–3] The resistant clones are thought to be generated through either intrinsic genetic instability resulting in tumor cell heterogeneity (TCH) or a cancer stem cell (CSC) population.[4–7] The resistant clones allow for regrowth of the cancer cell population after treatment insult. There is a growing body of evidence that the phenomenon of therapeutic resistance may be explained by a poorly recognized but distinct cell state. This cell state is documented as the nonproliferating polyaneuploid cancer cell (PACC) state, induced by tumor microenvironmental (intrinsic) or therapeutic (extrinsic) stress.[8–10] A doubling of a cancer cell's aneuploid genome combined with an exit from the cell cycle enables the PACC state. The cell state can exist for an extended period of time. In response to stress, a subset of cancer cells enters the PACC state by accessing an evolutionary or developmental polyploidization program. Once that stress is relieved, cells in the PACC state can act as CSCs by undergoing depolyploidization and repopulating the tumor cell population. The role of the PACC state for therapeutic resistance adds to those of CSC and TCH. Identifying cells in the PACC state in patients may have important diagnostic, prognostic, and therapeutic implications.

Large pleomorphic cancer cells with irregular nuclei have been documented in histopathologic specimens of multiple tumor types since the 1800s.[11] These cells have been reported utilizing a variety of names: polyaneuploid cancer cells (PACCs), polyploid giant cancer cells (PGCCs), giant cancer cells (GCCs), multinucleated GCCs, blastomere-like cancer cells, osteoclast-like cancer cells, cells in an embryonic diapause, pleomorphic giant cells, large stem cells, and persister cells.[12–23] Recent data indicate that these cells do not represent a different type of cancer cell within the heterogeneous tumor cell population, but rather a specific nonproliferative, polyaneuploid cell state.[8–10] In response to therapeutic stress, this cell state enables survival and is responsible for driving therapeutic resistance to nearly all available treatment regimens.

The presence of cells in the PACC state has been documented in virtually all cancer types, including adenocarcinomas, transitional cell tumors, squamous cell carcinomas, leukemias, lymphomas, glioblastomas, and sarcomas.[12,24–29] Most often observed in metastatic cancers or after treatment, their importance for patient prognosis has been understudied.[30,31] In glioma, Qu et al.[32] analyzed 76 patients and reported that the number of PACCs increased with the grade of tumors. In a study of 47 patients with anorectal melanoma, the number of PACCs was demonstrated to increase with tumor size.[33] In laryngeal cancer, Liu et al.[34] analyzed the presence of PGCCs in 102 patients and found that patients with high expression of PGCCs had a poorer prognosis. In breast cancer, Fei et al.[30] analyzed 167 histopathologic specimens, including benign tissue, primary breast tumors, and lymph node metastases, and found the highest number of PGCCs in the lymph node metastases of breast cancer patients. In a study of 30 patients, Gerashchenko et al.[35] reported that breast tumors with a higher proportion of polyploid cells were a marker of poor response to neoadjuvant chemotherapy. Lv et al.[36] investigated the presence of PGCCs with budding in 80 patients with serous ovarian tumors and found that the presence of PGCCs in the primary tumor correlated with metastasis. Zhang et al.[37] examined tissue from 159 patients with colorectal cancer and demonstrated that the presence of PGCCs with budding increased as tumors became more dedifferentiated.

The presence of cancer cells in the PACC state has been reported in prostate cancer (PCa).[12,38] In an autopsy study of PCa patients who had failed multiple lines of therapy, Mannan et al.[39] reported the presence of multiple cells with highly irregular polylobulated nuclei or multiple pleomorphic nuclei. Alharbi et al.[40] reported a series of 30 patients with a rare variant of PCa with focal pleomorphic giant cell features that were extremely aggressive and associated with poor outcomes. This study was undertaken to systematically assess the presence and importance of cells in the PACC state in men who underwent radical prostatectomy with curative intent to treat their presumed localized PCa.

2 | MATERIALS AND METHODS

2.1 | Patients

Men with National Comprehensive Cancer Network intermediate- or high-risk PCa who underwent radical prostatectomy at Johns Hopkins Hospital from 2007 to 2015 and who did not receive neoadjuvant treatment were identified from the Institutional Review Board-approved Brady Urological Institute Radical Prostatectomy database. Intermediate risk was defined as clinical stage T2b–T2c, or

biopsy Gleason grade groups 2–3, or prostate-specific antigen (PSA) 10–20 ng/ml, and high risk was defined as biopsy Gleason grade groups 4–5 or clinical stage T3, or PSA > 20 ng/ml.[41] There were 3685 men with NCCN intermediate- or high-risk PCa with radical prostatectomy from 2007 to 2015 who did not receive neoadjuvant treatment. Of those, 2159 (59%) had complete follow-up for metastasis through 2015 and represented the pool from which the case–cohort sample was drawn.

2.2 | Case–cohort

Case–cohort was originally assembled to include as "cases" men with metastasis or with biochemical recurrence (BCR) with a rapid PSA doubling time (<10 months) and who were also considered to be at high risk of metastasis.[42] From the cohort of 2159 patients, a subcohort of 244 patients was selected, and 115 cases (73 with BCR and rapid PSA doubling time, and 42 with metastasis). Tissue samples from these men were analyzed for PACC; samples from 307 men were informative for PACC. To focus specifically on the risk of metastasis as the outcome of interest, we excluded 65 "men with BCR and rapid PSA doubling time but without metastasis who were included as "cases" in the original case–cohort. This resulted in a subcohort of 209 patients (including eight metastasis cases), and 30 metastasis cases not in the subcohort, all of whom were informative for PACCs.

2.3 | Tissue microarrays (TMAs)

Prostate TMAs were prepared from formalin-fixed paraffin-embedded blocks of the radical prostatectomy specimens. A total of 2807 tissue samples of matched normal/benign and cancer were arrayed in nine TMA blocks. These TMAs were all constructed as described[42–45] from the index tumor (highest grade) with a 3–4-fold sampling redundancy. On hematoxylin and eosin (H&E)-stained tissue sections and TMA sections, identifying PACCs is difficult since they often have indistinct cell membranes, thus making it difficult to distinguish "pseudo" multinucleation from the real ones. Also, unlike many other types of adenocarcinoma and poorly differentiated carcinomas (e.g., high-grade urothelial carcinomas, nonsmall cell lung carcinomas), easily recognizable multinucleated or bizarrely enlarged nuclei are not readily apparent in the vast majority of even very high-grade cases. Therefore, we used immunohistochemistry against EpCAM (mouse monoclonal antibody; ab7504; Abcam) on these TMAs to visualize the epithelial cell membranes. All TMA slides were scanned on a Hamamatsu Nanozoomer and imported into Concentriq (from Proscia). The whole slide scan files were evaluated by two pathologists (L. T. and A. M. D. M.). PACCs were defined as large multinucleated or polylobated cells that are at least three times the size of a neighboring tumor cell as assessed by visual inspection.[39] The presence of PACCs and the number of PACCs on each core were noted.

2.4 | Statistical analyses

Descriptive statistics were used to compare cases and subcohort, including Wilcoxon's rank-sum test for continuous variables and Fisher's exact test or χ^2 test for categorical variables. Correlations between PACCs and clinical variables were performed with linear regression or analysis of variance. The primary outcome was metastasis confirmed by imaging, and metastasis-free survival (MFS) was measured from the date of radical prostatectomy. Multivariable Cox proportional hazards regression models, with weights for the case–cohort design and robust variance estimator defined by Barlow[46] were fit to MFS to evaluate the hazard ratio (HR) and 95% confidence interval (CI) associated with PACCs, adjusted for established prognostic factors or Cancer of the Prostate Risk Assessment Postsurgical (CAPRA-S) score. The CAPRA-S score combines the pathologic Gleason score, pathologic stage, surgical margin status, and preoperative PSA in an algorithm with values ranging from 0 to 12; scores of 6 or higher are considered to indicate a high risk of BCR.[47] Improvement in multivariable model fit for the addition of PACCs was assessed with the pseudo-likelihood ratio test for the change in deviance from the full versus the reduced model.[48] In addition to the primary outcome of MFS, follow-up for the development of metastatic castration-resistant PCa (mCRPC) was available for 33 of the men with metastases. Time from diagnosis of metastasis to mCRPC was analyzed using standard proportional hazards regression, and improvement in model fit was assessed with the likelihood ratio test. All analyses were performed with SAS v. 9.4 (SAS Institute).

3 | RESULTS

Since the great majority of prostatic adenocarcinomas do not frequently show bizarre nuclear atypia with extremely large nuclei or multinucleation that is readily apparent by H&E staining, we performed IHC against EpCAM to facilitate the recognition of cellular plasma membranes. This greatly helped in the ability to confidently identify PACCs (Figure 1 and Supporting Information: Figure 1), which in this study were limited to cells with multiple nuclei bounded by a single plasma membrane. Table 1 compares the metastasis cases to men without metastasis. Cases had the expected higher risk profile, differing significantly for all variables except age. Although many patient tumor samples had none, PACCs were significantly more frequent in cases with metastasis, 20 of 38 cases (52.6%), versus 68 of 201 (33.8%) controls, $p = 0.029$.

The total number of PACCs and the total number of cores with PACCs were significantly correlated with increasing Gleason score ($p = 0.0004$) and increasing CAPRA-S ($p = 0.004$), but no other variables.

In univariate proportional hazards models of MFS, year of surgery, Gleason score (9–10 vs. 7–8), pathology stage, CAPRA-S, total PACCs, and cores positive for PACCs (both evaluated as a continuous variable or dichotomized at ≥1 vs. 0) were all statistically

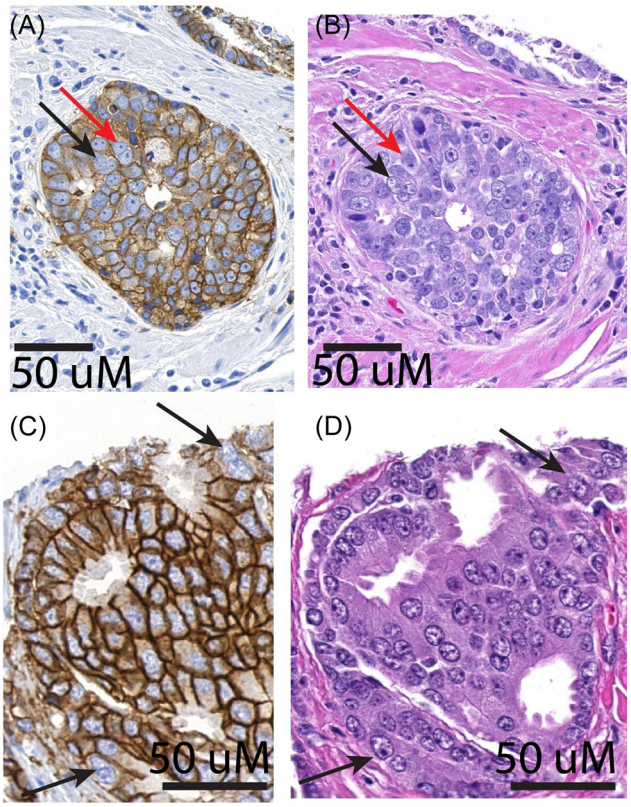

FIGURE 1 TMA spot stained with EpCAM to distinguish cells in the PACC state. TMA was stained with EpCAM (A, C) and H&E (B, D) on adjacent slices. Arrow indicates a cell in the PACC state, determined from the EpCAM stain as a cell with two nuclei or a lobulated nucleus within a single plasma membrane. The H&E in the same region does not adequately distinguish between cell–cell boundaries; thus, it is difficult to discern if there is multinucleation. H&E, hematoxylin and eosin; PACC, polyaneuploid cancer cell; TMA, tissue microarray. [Color figure can be viewed at wileyonlinelibrary.com]

significant (Table 2). Note that dichotomizing total PACCs and cores positive for PACCs gave the same distribution so that the HRs, 95% CIs, and *p* values are the same.

The multivariable models with PACCs that gave the best fit included CAPRA-S. Adding either total PACCs or cores positive for PACCs (both expressed as a continuous variable) to CAPRA-S significantly improved model fit compared to CAPRA-S alone, based on the pseudo-likelihood ratio test (Table 3). The best-fitting model included total PACCs, HR = 2.00 (95% CI: 1.40, 2.87), and CAPRA-S, HR = 2.51 (95% CI: 1.81, 3.48).

Among 38 patients with metastases, 32 had complete data on PGCCs, CAPRA-S, and time to mCRPC. Table 4 shows univariate analyses for CAPRA-S and total PACCs (expressed as a continuous variable), and the multivariable model of total PACCs and CAPRA-S. Cores positive for PACCs were not statistically significant in a univariate model or adjusted for CAPRA-S (data not shown). Total PACCs were statistically significant in the univariate model, HR = 1.23 (95% CI: 1.06, 1.43), $p = 0.007$, but was no longer significant when adjusted for CAPRA-S, HR = 1.17 (95% CI: 0.995, 1.38), $p = 0.057$. The small sample size resulted in a lack of statistical power, which may have influenced the result.

4 | DISCUSSION

The major cause of death related to PCa is the development of therapy-resistant metastatic disease. The possible mechanisms of therapy resistance in PCa have been broadly investigated with multiple candidates such as *SOX2* activation, *MYC* and *RAS* coactivation, and *ERG* gene rearrangements.[49–51] However, the PACC state may represent an inclusive and unifying explanation for therapy resistance mechanisms, that is, underrecognized. This cell state is induced by the tumor microenvironment or therapeutic stress, can exist for an extended period of time, and can act as a CSC by undergoing depolyploidization and repopulating the tumor cell population when stress is relieved. To systematically study this phenomenon, one needs to go back to the fundamental approach to tumor pathogenesis: cell morphology.

The PACC state has two defining characteristics: polyploidy and relatively large size. Polyploidy does not necessarily mean "multinucleation" and can be pronounced as a single large nucleus; however, multinucleated cells are often polyploid. Because of the increased genomic content, polyploid cells are physically larger than the neighboring tumor cells.[12] The presence of cells in the PACC state has been shown to be associated with worse prognosis, higher tumor grade, poor differentiation, and advanced disease stage in various tumor types including PCa.[30,32,34,36,37,40] There is also evidence in castration-resistant PCa that cells in the PACC state drive resistance to taxane-based chemotherapy.[52]

In this study, we investigated the presence of cells in the PACC state and their clinical importance in patients who underwent radical prostatectomy with curative intent to treat their presumed localized PCa. Our findings show that the number of PACCs and the number of cores positive for PACCs are statistically significant prognostic factors for MFS, after adjusting for CAPRA-S, in a case–cohort of intermediate- or high-risk men who underwent radical prostatectomy. In addition, despite the small number of men with complete data to evaluate time to mCRPC, the total number of cells in the PACC state was a statistically significant predictor of mCRPC in univariate analysis and suggested a prognostic effect even after adjusting for CAPRA-S. To our knowledge, our study is the first to describe the adverse clinical implications of the presence and of cells in the PACC state in a stratified cohort of PCa patients based on the metastasis status. Assessing the prognostic value of PACCs for mCRPC by employing a larger cohort, prospective analyses of the predictive value of PACCs for adverse clinical outcome, and ultimately, whole-genome and RNA-sequencing of the genetic material of these cells by using microdissection methods are of interest in understanding the biology of the PACC state. It should be pointed out, however, that none of the PACC-associated variables in Table 2 was as strong as the Gleason score, pathological stage, or CAPRA-S.

TABLE 1 Characteristics of patients with or without metastases ($n = 239$)

Variables	Metastases ($n = 38$)	No metastases ($n = 201$)	p Value
Age, median (IQR)	59 (56–63)	59 (54–65)	0.747
PSA, median (IQR)	7.0 (5.3–8.7)	5.5 (4.3–8.3)	0.028
Race, *n* (%)			
White	32 (16.8)	159 (83.3)	0.167
Black	6 (20.7)	23 (79.3)	
Other	0 (0)	16 (100.0)	
Prostatectomy year, median (IQR)	2008 (2007–2009)	2009 (2008–2011)	0.014
Prostatectomy Gleason score, *n* (%)			<0.0001
6	0 (0	43 (100.0	
3 + 4	1 (1.1)	88 (98.9)	
4 + 3	9 (17.3)	43 (82.7)	
8	6 (30.0)	14 (70.0)	
9–10	22 (68.8)	10 (31.2)	
Pathology stage, *n* (%)			<0.0001
Organ confined	6 (4.8)	118 (95.2)	
Extraprostatic extension	10 (13.3)	65 (86.7)	
Seminal vesicle involvement	10 (45.5)	12 (54.5)	
Lymph node involvement	12 (85.7)	2 (14.3)	
Surgical margins, *n* (%)			0.002
Negative	23 (12.2)	165 (87.8)	
Positive	14 (30.4)	32 (69.6)	
NCCN risk, *n* (%)			0.0001
Intermediate	17 (9.6)	160 (90.4)	
High	15 (31.3)	33 (68.8)	
Salvage treatment, *n* (%)			<0.0001
None	21 (11.0)	170 (89.0)	
ADT only	4 (66.7)	2 (33.3)	
Radiation only	8 (32.0)	17 (68.0)	
ADT + radiation	5 (35.7)	9 (64.3)	
CAPRA-S, median (IQR)	7 (4–8)	2 (1–4)	<0.0001
Cores with PACCs, median (IQR)	1 (0–2)	0 (0–1)	0.016
Cores with PACCs, *n* (%)[a]			0.029
0	18 (11.9)	133 (88.1)	
≥1	20 (22.7)	68 (77.3)	
Total number of PACCs, median (IQR)	1 (0–3)	0 (0–1)	0.011
Total number of PACCs, *n* (%)[a]			0.029
0	18 (11.9)	133 (88.2)	
≥1	20 (22.7)	68 (77.3)	

Abbreviations: ADT, androgen deprivation therapy; CAPRA-S, Cancer of the Prostate Risk Assessment Postsurgical; IQR, interquartile range; NCCN, National Comprehensive Cancer Network; PACCs, polyaneuploid cancer cells.

[a]Binary classification of total PACCs and cores with PACCs gives the same distribution

TABLE 2 Univariate proportional hazards models of metastasis-free survival in a case–cohort of intermediate- and high-risk men

Variables	HR (95% CI)	*p* Value
Year of surgery	1.50 1.12, 2.02)	0.007
Age	0.99 (0.93, 1.05)	0.671
PSA (per 1 ng/ml)	1.03 (0.996, 1.07)	0.079
Gleason score		<0.0001
7–8	1.0	
9–10	13.48 (5.40, 33.65)	
Pathologic stage		<0.0001
Organ-confined	1.0	
Extraprostatic extension	3.95 (1.27, 12.32)	
Seminal vesicle involvement	17.05 (3.83, 75.83)	
Lymph node involvement	61.46 (11.58, 326.33)	
CAPRA-S (per 1 unit)	2.32 (1.79, 3.01)	<0.0001
Total PACCs (per 1 PACC)	1.38 (1.09, 1.73)	0.006
Total PACCs (≥1 vs. 0)[a]	2.70 (1.24, 5.86)	0.012
Cores with PACCs (per 1 core)	1.40 (1.004, 1.94)	0.047
Cores with PACCs (≥1 vs. 0)[a]	2.70 (1.24, 5.86)	0.012

Abbreviations: CAPRA-S, Cancer of the Prostate Risk Assessment Postsurgical; CI, confidence interval; HR, hazard ratio; PACCs, polyaneuploid cancer cells.

[a]Binary classification of total PACCs and cores with PACCs gives the same distribution, so results from the proportional hazards model are also the same.

One of the main challenges in this study was to accurately identify cells in the PACC state. We found the EpCAM stain is helpful in visualizing the larger and atypical tumoral cells and increasing our ability to detect PACCs of various morphologies. It is clear that using a specific biomarker to highlight PACCs would be the ideal approach in studying these cells. However, there are currently no biomarkers for the PACC state, either for monitoring in vivo or for isolation, and we believe this should be an area for future research.

Another challenge that might have affected the results of this study is tumor heterogeneity, which has long been known to be present in PCa,[53] given the fact that we employed TMAs to detect PACCs in our cohort. Although we applied a 3–4-fold sampling redundancy to reduce the margin of error, it is clear that the results of this study might have been affected by underrepresentation of PACCs because of the heterogeneous nature of PCa.

We did not determine the incremental improvement in the concordance index associated with adding PACCs to the model containing CAPRA-S because we are not aware of a validated approach to doing so for a case-cohort study design. However, it has been shown that if a variable is a statistically significant addition to a multivariable model, it is mathematically equivalent to demonstrating a significant improvement in model performance and that the test for significance of adding the variable has greater statistical power than a test of increase in concordance index. Since PACCs were statistically significant when added to a model with CAPRA-S, it implies that adding the biomarker significantly improved model performance.[54,55]

Because of its important role in disease resistance, we believe it is important to eliminate the PACC state during the treatment of

TABLE 3 Multivariable proportional hazards models of metastasis-free survival in a case–cohort of intermediate- and high-risk men

Variables	HR (95% CI)	*p* Value	*p* Value for increase in PLRT[a] compared to CAPRA-S alone
Model 1			
CAPRA-S (per 1 unit)	2.50 (1.81, 3.46)	<0.0001	<0.0001
Total PACCs (per 1 PACC)	2.00 (1.40, 2.85)	0.0001	
Model 2			
CAPRA-S (per 1 unit)	2.23 (1.73, 2.88)	<0.0001	0.076
Total PACCs (≥1 vs. 0)[b]	1.97 (0.54, 7.24)	0.306	
Model 3			
CAPRA-S (per 1 unit)	2.35 (1.79, 3.09)	<0.0001	0.0003
Cores with PACCs (per 1 core)	2.15 (1.23, 3.78)	0.007	
Model 4			
CAPRA-S (per 1 unit)	2.23 (1.73, 2.88)	<0.0001	0.076
Cores with PACCs (≥1 vs. 0)[b]	1.97 (0.54, 7.24)	0.306	

Abbreviations: CAPRA-S, Cancer of the Prostate Risk Assessment Postsurgical; CI, confidence interval; HR, hazard ratio; PACCs, polyaneuploid cancer cells; PLRT, pseudo-likelihood ratio test.

[a]The pseudo-likelihood ratio test is based on the change in deviance when one of the PACC variables is added to a model of CAPRA-S alone.

[b]Binary classification of total PACCs and cores with PACCs gives the same distribution, so results from the proportional hazards model are also the same.

TABLE 4 Univariate and multivariable proportional hazards models of time from metastasis to mCRPC in a cohort of intermediate- and high-risk men with metastasis ($n = 32$)

Variables	HR (95% CI)	*p* Value	*p* Value for increase in LRT[a] compared to CAPRA-S alone
Univariate			
CAPRA-S (per 1 unit)	1.14 (0.97, 1.33)	0.106	n/a
Total PACCs (per 1 PACC)	1.22 (1.05, 1.42)	0.011	n/a
Multivariable			
CAPRA-S (per 1 unit)	1.08 (0.93, 1.27)	0.322	0.075
Total PACCs (per 1 PACC)	1.17 (0.995, 1.38)	0.057	

Abbreviations: CAPRA-S, Cancer of the Prostate Risk Assessment Postsurgical; CI, confidence interval; HR, hazard ratio; LRT, likelihood ratio test; n/a, not applicable; PACC, polyaneuploid cancer cells.

[a]The likelihood ratio test is based on the change in deviance when total PACCs are added to a model of CAPRA-S alone.

aggressive PCa patients. However, there are no agents to specifically target these cells to date. Their unique biology and phenotype may create therapeutic opportunities as they may have unexpected vulnerabilities. This is a critical area of research in combination with molecular analysis of their genome.

Although there is scarce knowledge about the biology of cells the PACC state, we and others have shown their likely role in mediating disease resistance. We present additional evidence that they are significant prognostic factors for metastasis in patients with PCa who underwent radical prostatectomy with curative intent to treat their presumed localized PCa.

ACKNOWLEDGMENTS

This work was supported by NCI Grants U54CA143803, CA163124, CA093900, and CA143055, and the Prostate Cancer Foundation to Kenneth J. Pienta; NCI Grant P50CA058236, US Department of Defense CDMRP/PCRP (W81XWH-21-0-373), the Patrick C. Walsh Prostate Cancer Research Fund to Bruce J. Trock; US Department of Defense Prostate Cancer Biospecimen Network Site, Grant/Award Number: W81XWH-18-2-0015; National Cancer Institute, Grant/Award Numbers: MCL U01 CA1936390 P30 CA006973; SPORE in Prostate Cancer, Grant/Award Number: P50CA58236; The Prostate Cancer Foundation to Angelo M. De Marzo; US Department of Defense CDMRP/PCRP (W81XWH-20-10353), the Patrick C. Walsh Prostate Cancer Research Fund, and the Prostate Cancer Foundation to Sarah R. Amend.

CONFLICTS OF INTEREST

Kenneth J. Pienta is a consultant for CUE Biopharma, Inc. and holds an equity interest in Keystone Biopharma, Inc. Bruce J. Trock has research grants through Johns Hopkins from MDxHealth, Inc., Myriad Genetics, Inc., Opko Health, Inc., and Exact Sciences, Inc. Angelo M. De Marzo is a consultant for Merck, Inc. and Cepheid Inc. He has sponsored research support from Janssen and Myriad Genetics Inc. Sarah R. Amend holds an equity interest in Keystone Biopharma, Inc. The remaining author declares no conflicts of interest.

DATA AVAILABILITY STATEMENT

All data are available upon request.

ORCID

Angelo M. De Marzo http://orcid.org/0000-0003-4847-5307
Sarah R. Amend http://orcid.org/0000-0002-5606-1262

REFERENCES

1. Cree IA, Charlton P. Molecular chess? Hallmarks of anti-cancer drug resistance. *BMC Cancer*. 2017;17(1):10.
2. Nikolaou M, Pavlopoulou A, Georgakilas AG, Kyrodimos E. The challenge of drug resistance in cancer treatment: a current overview. *Clin Exp Metastasis*. 2018;35(4):309-318.
3. Aleksakhina SN, Kashyap A, Imyanitov EN. Mechanisms of acquired tumor drug resistance. *Biochim Biophys Acta*. 2019;1872(2):188310.
4. Burrell RA, Swanton C. Tumour heterogeneity and the evolution of polyclonal drug resistance. *Mol Oncol*. 2014;8(6):1095-1111.
5. Shibue T, Weinberg RA. EMT, CSCs, and drug resistance: the mechanistic link and clinical implications. *Nat Rev Clin Oncol*. 2017;14(10):611-629.
6. Dagogo-Jack I, Shaw AT. Tumour heterogeneity and resistance to cancer therapies. *Nat Rev Clin Oncol*. 2018;15(2):81-94.
7. Luo M, Brooks M, Wicha M. Epithelial–mesenchymal plasticity of breast cancer stem cells: implications for metastasis and therapeutic resistance. *Curr Pharm Des*. 2015;21(10):1301-1310.
8. Pienta KJ, Hammarlund EU, Axelrod R, Brown JS, Amend SR. Poly-aneuploid cancer cells promote evolvability, generating lethal cancer. *Evol Appl*. 2020;13(7):1626-1634.
9. Pienta KJ, Hammarlund EU, Austin RH, Axelrod R, Brown JS, Amend SR. Cancer cells employ an evolutionarily conserved polyploidization program to resist therapy. *Semin Cancer Biol*. 2022;81:145-159. doi:10.1016/j.semcancer.2020.11.016
10. Pienta KJ, Hammarlund EU, Brown JS, Amend SR, Axelrod RM. Cancer recurrence and lethality are enabled by enhanced survival and reversible cell cycle arrest of polyaneuploid cells. *Proc Natl Acad Sci USA*. 2021;118(7):e2020838118. doi:10.1073/pnas.2020838118
11. Virchow R. Cellular pathology, as based upon physiological and pathological histology Classics of Medicine Library Special Edition. In: De Witt RM ed. Twenty lectures delivered in the Pathological Institute of Berlin during the months of February, March and April, Leslie B. Adams, Jr. ; 1858. 1860:xxvi, 27–554.

12. Amend SR, Torga G, Lin KC, et al. Polyploid giant cancer cells: unrecognized actuators of tumorigenesis, metastasis, and resistance. *Prostate*. 2019;79(13):1489-1497.
13. Mirzayans R, Andrais B, Murray D. Roles of polyploid/multinucleated giant cancer cells in metastasis and disease relapse following anticancer treatment. *Cancers*. 2018;10(4):118. doi:10.3390/cancers10040118
14. Chen J, Niu N, Zhang J, et al. Polyploid giant cancer cells (PGCCs): the evil roots of cancer. *Curr Cancer Drug Targets*. 2019;19(5):360-367.
15. Illidge T. Polyploid giant cells provide a survival mechanism for p53 mutant cells after DNA damage. *Cell Biol Int*. 2000;24(9):621-633.
16. Niu N, Mercado-Uribe I, Liu J. Dedifferentiation into blastomere-like cancer stem cells via formation of polyploid giant cancer cells. *Oncogene*. 2017;36(34):4887-4900.
17. Brooks PJ, Glogauer M, McCulloch CA. An overview of the derivation and function of multinucleated giant cells and their role in pathologic processes. *Am J Pathol*. 2019;189(6):1145-1158.
18. Moein S, Adibi R, da Silva Meirelles L, Nardi NB, Gheisari Y. Cancer regeneration: polyploid cells are the key drivers of tumor progression. *Biochim Biophys Acta*. 2020;1874(2):188408.
19. Weihua Z, Lin Q, Ramoth AJ, Fan D, Fidler IJ. Formation of solid tumors by a single multinucleated cancer cell. *Cancer*. 2011;117(17):4092-4099.
20. Rajaraman R, Guernsey DL, Rajaraman MM, Rajaraman SR. Stem cells, senescence, neosis and self-renewal in cancer. *Cancer Cell Int*. 2006;6:25.
21. Dhimolea E, de Matos Simoes R, Kansara D, et al. An embryonic diapause-like adaptation with suppressed myc activity enables tumor treatment persistence. *Cancer Cell*. 2021;39(2):240-256.
22. Rehman SK, Haynes J, Collignon E, et al. Colorectal cancer cells enter a diapause-like DTP state to survive chemotherapy. *Cell*. 2021;184(1):226-242.e21.
23. Liu J, Niu N, Li X, Zhang X, Sood AK. The life cycle of polyploid giant cancer cells and dormancy in cancer: opportunities for novel therapeutic interventions. *Semin Cancer Biol*. 2022;81:132-144. doi:10.1016/j.semcancer.2021.10.005
24. Saini G, Joshi S, Garlapati C, et al. Polyploid giant cancer cell characterization: new frontiers in predicting response to chemotherapy in breast cancer. *Semin Cancer Biol*. 2022;81:220-231. doi:10.1016/j.semcancer.2021.03.017
25. Imai Y, Morishita S, Ikeda Y, et al. Immunohistochemical and molecular analysis of giant cell carcinoma of the pancreas: a report of three cases. *Pancreas*. 1999;18(3):308-315.
26. Mosnier JF, Balique JG. Pleomorphic giant cell carcinoma of the esophagus with coexpression of cytokeratin and vimentin and neuroendocrine differentiation. *Arch Pathol Lab Med*. 2000;124(1):135-138.
27. O'Connor RC, Hollowell CMP, Laven BA, Yang XJ, Steinberg GD, Zagaja GP. Recurrent giant cell carcinoma of the bladder. *J Urol*. 2002;167(4):1784.
28. Shen R, Wen P. Clear cell renal cell carcinoma with syncytial giant cells: a case report and review of the literature. *Arch Pathol Lab Med*. 2004;128(12):1435-1438.
29. Schwartz HS, Eskew JD, Butler MG. Clonality studies in giant cell tumor of bone. *J Orthop Res*. 2002;20(2):387-390.
30. Fei F, Zhang D, Yang Z, et al. The number of polyploid giant cancer cells and epithelial–mesenchymal transition-related proteins are associated with invasion and metastasis in human breast cancer. *J Exp Clin Cancer Res*. 2015;34:158.
31. Zhang S, Mercado-Uribe I, Xing Z, Sun B, Kuang J, Liu J. Generation of cancer stem-like cells through the formation of polyploid giant cancer cells. *Oncogene*. 2014;33(1):116-128.
32. Qu Y, Zhang L, Rong Z, He T, Zhang S. Number of glioma polyploid giant cancer cells (PGCCs) associated with vasculogenic mimicry formation and tumor grade in human glioma. *J Exp Clin Cancer Res*. 2013;32:75.
33. Liu G, Wang Y, Fei F, et al. Clinical characteristics and preliminary morphological observation of 47 cases of primary anorectal malignant melanomas. *Melanoma Res*. 2018;28(6):592-599.
34. Liu HT, Xia T, You YW, et al. Characteristics and clinical significance of polyploid giant cancer cells in laryngeal carcinoma. *Laryngoscope Investig Otolaryngol*. 2021;6(5):1228-1234.
35. Gerashchenko BI, Salmina K, Eglitis J, Huna A, Grjunberga V, Erenpreisa J. Disentangling the aneuploidy and senescence paradoxes: a study of triploid breast cancers non-responsive to neoadjuvant therapy. *Histochem Cell Biol*. 2016;145(4):497-508.
36. Lv H, Shi Y, Zhang L, et al. Polyploid giant cancer cells with budding and the expression of cyclin E, S-phase kinase-associated protein 2, stathmin associated with the grading and metastasis in serous ovarian tumor. *BMC Cancer*. 2014;14:576.
37. Zhang D, Yang X, Yang Z, et al. Daughter cells and erythroid cells budding from PGCCs and their clinicopathological significances in colorectal cancer. *J Cancer*. 2017;8(3):469-478.
38. Lopez-Beltran A, Eble JN, Bostwick DG. Pleomorphic giant cell carcinoma of the prostate. *Arch Pathol Lab Med*. 2005;129(5):683-685.
39. Mannan R, Wang X, Bawa PS, et al. Polypoidal giant cancer cells in metastatic castration-resistant prostate cancer: observations from the Michigan Legacy Tissue Program. *Med Oncol*. 2020;37(3):16.
40. Alharbi AM, De Marzo AM, Hicks JL, Lotan TL, Epstein JI. Prostatic adenocarcinoma with focal pleomorphic giant cell features: a series of 30 cases. *Am J Surg Pathol*. 2018;42(10):1286-1296.
41. Mohler J, Bahnson RR, Boston B, et al. The NCCN Prostate Cancer Clinical Practice Guidelines in Oncology. *J Nat Comp Cancer Netw*. 2010;8(2):200.
42. Vidal I, Zheng Q, Hicks JL, et al. GSTP1 positive prostatic adenocarcinomas are more common in Black than White men in the United States. *PLoS One*. 2021;16(6):e0241934.
43. Chaux A, Peskoe SB, Gonzalez-Roibon N, et al. Loss of PTEN expression is associated with increased risk of recurrence after prostatectomy for clinically localized prostate cancer. *Mod Pathol*. 2012;25(11):1543-1549.
44. Gurel B, Iwata T, M Koh C, et al. Nuclear MYC protein overexpression is an early alteration in human prostate carcinogenesis. *Mod Pathol*. 2008;21(9):1156-1167.
45. Faith DA, Isaacs WB, Morgan JD, et al. Trefoil factor 3 overexpression in prostatic carcinoma: prognostic importance using tissue microarrays. *Prostate*. 2004;61(3):215-227.
46. Barlow WE, Ichikawa L, Rosner D, Izumi S. Analysis of case-cohort designs. *J Clin Epidemiol*. 1999;52(12):1165-1172.
47. Cooperberg MR, Hilton JF, Carroll PR. The CAPRA-S score: a straightforward tool for improved prediction of outcomes after radical prostatectomy. *Cancer*. 2011;117(22):5039-5046.
48. Langholz B, Jiao J. Computational methods for case-cohort studies. *Comput Stat & Data Anal*. 2007;51:3737-3748.
49. de Wet L, Williams A, Gillard M, et al. SOX2 mediates metabolic reprogramming of prostate cancer cells. *Oncogene*. 2022;41(8):1190-1202.
50. Arriaga JM, Panja S, Alshalalfa M, et al. A MYC and RAS co-activation signature in localized prostate cancer drives bone metastasis and castration resistance. *Nature Cancer*. 2020;1(11):1082-1096.
51. Udager AM, Shi Y, Tomlins SA, et al. Frequent discordance between ERG gene rearrangement and ERG protein expression in a rapid autopsy cohort of patients with lethal, metastatic,

castration-resistant prostate cancer. *Prostate*. 2014;74(12):1199-1208.
52. Mittal K, Donthamsetty S, Kaur R, et al. Multinucleated polyploidy drives resistance to docetaxel chemotherapy in prostate cancer. *Br J Cancer*. 2017;116(9):1186-1194.
53. Haffner MC, Zwart W, Roudier MP, et al. Genomic and phenotypic heterogeneity in prostate cancer. *Nat Rev Urol*. 2021;18(2):79-92.
54. Pepe MS, Kerr KF, Longton G, Wang Z. Testing for improvement in prediction model performance. *Stat Med*. 2013;32(9):1467-1482.
55. Vickers AJ, Cronin AM, Begg CB. One statistical test is sufficient for assessing new predictive markers. *BMC Med Res Methodol*. 2011;11(1):13.

SUPPORTING INFORMATION

Additional supporting information can be found online in the Supporting Information section at the end of this article.

How to cite this article: Trabzonlu L, Pienta KJ, Trock BJ, De Marzo AM, Amend SR. Presence of cells in the polyaneuploid cancer cell (PACC) state predicts the risk of recurrence in prostate cancer. *The Prostate*. 2023;83:277-285. doi:10.1002/pros.24459

Neoplasia 42 (2023) 100906

Contents lists available at ScienceDirect

Neoplasia

journal homepage: www.elsevier.com/locate/neo

Original Research

Nuclear morphology predicts cell survival to cisplatin chemotherapy

Chi-Ju Kim[a,1,*], Anna LK Gonye[a,b,1], Kevin Truskowski[a,b], Cheng-Fan Lee[a], Yoon-Kyoung Cho[c,d], Robert H. Austin[e], Kenneth J. Pienta[a,b], Sarah R. Amend[a,b,*]

[a] Cancer Ecology Center, The Brady Urological Institute, Johns Hopkins School of Medicine, 600 N. Wolfe St., Baltimore, MD 21287, USA
[b] Cellular and Molecular Medicine Graduate Program, Johns Hopkins School of Medicine, 600 N. Wolfe St., Baltimore, MD 21287, USA
[c] Department of Biomedical Engineering, Ulsan National Institute of Science and Technology, Building 103, Ulsan 44919, Republic of Korea
[d] Center for Soft and Living Matter, Institute for Basic Science, Ulsan 44919, Republic of Korea
[e] Department of Physics, Princeton University, Jadwin Hall, Washington Rd., Princeton, NJ 08544, USA

ARTICLE INFO

Keywords:
Cancer therapy resistance
Polyaneuploid cancer cell (PACC) state
Nuclear morphology
Polyploidy

ABSTRACT

The emergence of chemotherapy resistance drives cancer lethality in cancer patients, with treatment initially reducing overall tumor burden followed by resistant recurrent disease. While molecular mechanisms underlying resistance phenotypes have been explored, less is known about the cell biological characteristics of cancer cells that survive to eventually seed the recurrence. To identify the unique phenotypic characteristics associated with survival upon chemotherapy exposure, we characterized nuclear morphology and function as prostate cancer cells recovered following cisplatin treatment. Cells that survived in the days and weeks after treatment and resisted therapy-induced cell death showed increasing cell size and nuclear size, enabled by continuous endocycling resulting in repeated whole genome doubling. We further found that cells that survive after therapy release were predominantly mononucleated and likely employ more efficient DNA damage repair. Finally, we show that surviving cancer cells exhibit a distinct nucleolar phenotype and increased rRNA levels. These data support a paradigm where soon after therapy release, the treated population mostly contains cells with a high level of widespread and catastrophic DNA damage that leads to apoptosis, while the minority of cells that have successful DDR are more likely to access a pro-survival state. These findings are consistent with accession of the polyaneuploid cancer cell (PACC) state, a recently described mechanism of therapy resistance and tumor recurrence. Our findings demonstrate the fate of cancer cells following cisplatin treatment and define key cell phenotypic characteristics of the PACC state. This work is essential for understanding and, ultimately, targeting cancer resistance and recurrence.

Introduction

Once cancer has metastasized, it is incurable because tumors evolve resistance to virtually all systemically administered anticancer therapies. The cells that eventually seed a resistant recurrence must first survive the initial chemotherapeutic insult. While several non-mutually exclusive models exist to explain the predisposition of a cell population to survive therapy (e.g., tumor cell heterogeneity models, cancer stem cell models), less is known about the cell biology characteristics of surviving cells following therapy exposure. Cell morphology is representative of cellular phenotype and reflects the underlying biology of a cell. Abnormal nuclear morphology is often conspicuous in cancer cells [1,2] and variation in nuclear size and shape is a significant pathologic parameter that is used clinically for the diagnosis of various cancers [1]. Hyperabnormal nuclear morphologies, such as multilobulated and multinucleated nuclei, are highly associated with metastasis and recurrence [3–5]. Evaluating these cell morphological characteristics is critical to understanding the mechanisms enable cell survival following chemotherapy treatment and the eventual evolution of resistant recurrence.

Chemotherapeutic agents show utility in cancer because of their effects on rapidly proliferating cells, with specific effects on DNA replication machinery or cell division machinery. One underappreciated cellular mechanism to avoid cell death secondary to damage caused by chemotherapy is to skip mitosis and/or cytokinesis, thus not engaging the critical G2/M cell cycle checkpoint. Such mitotic skipping results in increased cellular contents, including increased nuclear size and genomic material, and is hypothesized to aid the cell in adapting to toxic environments such as therapeutic stress [6–9]. The increased genomic content may also help to prevent cells from undergoing cell cycle checkpoint-activated apoptosis due to DNA damage [4,6–15]. This

* Corresponding authors at: 600 North Wolfe Street, Marburg 121, Baltimore, MD 21287; USA.
E-mail addresses: ckim143@jhmi.edu (C.-J. Kim), samend2@jhmi.edu (S.R. Amend).
[1] These authors contributed equally to this work.

https://doi.org/10.1016/j.neo.2023.100906
Received 17 March 2023; Received in revised form 4 May 2023; Accepted 4 May 2023

amitotic cell cycle that leads to genomic duplication is accompanied by abnormal nuclear morphologies including large mononucleated, mononucleated and simultaneously lobulated, or multinucleated phenotypes [6–9,12–14].

DNA damage response (DDR) is a pathway to overcome the effect of chemotherapeutic agents such as cisplatin, a DNA poison. If cells are exposed to genotoxic stress, DDR machinery is activated to repair damaged DNA. In case of double-stranded DNA breaks, there are two DDR pathways including non-homologous end-joining (NHEJ) and homologous recombination (HR). DDR procedures commonly consist of two crucial steps: sensing damaged DNA lesions and recruiting DNA repair molecules. Gamma H2A.X (gH2AX) acts as an DNA damage sensing marker, and 53BP1 in NHEJ or BRCA1 in HR are active DNA repair molecules. These DDR machineries thus initially allow the cells to survive after chemotherapy treatment. Furthermore, successfully completed DDR may also prevent cell death at cell cycle checkpoints, which enables reactivation of cell cycles and prolongs their cellular life.

To define the life history of cells following chemotherapy treatment that continue to survive versus those that die after chemotherapy, we characterized nuclear morphology and function over time following release from treatment with cisplatin. We demonstrate that mononucleated, polyploid cells dominate the population of cells that survive following therapy and thus likely represent the cells that will eventually seed a therapeutically resistant population. These data indicate that cells that survive cisplatin treatment access a mononucleated state, continue to replicate DNA via endocycling, and retain high levels of active DNA damage repair machinery, while multinucleated cells eventually undergo cell death.

Materials and methods

Cell culture

PC3 cell line was originally purchased from ATCC (United States). Cells were maintained in RPMI-1640 with L-Glutamine (PC3; Gibco, #11875-093) with 10% FBS (Avantar, #97068-085) and 1% penicillin streptomycin (Gibco, #15140-122).

Treatment

Prior to drug treatment, the lethal dose 50 (LD50) values of three chemotherapeutics (cisplatin, docetaxel, and etoposide) were evaluated from dose response curves obtained via an alarmarBlue assay (VWR, #76285-554). Sub-confluent cultures of PC3 cells were treated with [LD50] cisplatin (6 μM; Millipore Sigma, #232120-50MG), docetaxel (5 nM; Cell Signaling Technology, #9886), or etoposide (25 μM; Cell Signaling Technology, #2200S) and cultured for 72 h under standard conditions. Large cells were then sterilely isolated via size-restricted filtration with a pluriStrainer® 15 μm cell strainer (pluriSelect, #45-50015-03) and replated for culturing.

Nuclear morphological analysis

Large cells were generated as described, isolated, and then cultured for 1, 5, 10, and 15 days following 72 h of drug treatment. 24 h prior to each timepoint, the cells were seeded into 35 mm IbiTreat μ-Dishes (Ibidi USA Inc., #81156) and incubated overnight. Samples were fixed in 10% formalin for 20 min, and permeabilized for 10 min in 0.2% Triton-X-100 in PBS. Permeabilized samples were blocked with 10% goat serum in PBS at room temperature for 30 min. Samples were then incubated overnight at 4°C with a lamin A/C primary antibody and secondary antibody (Table S1) for 1 h at room temperature. Samples were mounted with ProLong™ Diamond Antifade Mountant with DAPI (Invitrogen, #P36971) and images were acquired using a Zeiss Observer Z1 microscope/ZEN pro 2.0 software (Carl Zeiss Microscopy). Nuclear morphology (mono-nucleated vs. multi-nucleated) was manually discriminated and counted using Fiji [16].

Nucleolar morphological analysis

Cells were induced, seeded, fixed, permeabilized, and blocked as above. The samples were incubated with nucleolin and lamin A/C primary antibodies overnight at 4°C and a secondary antibody (Table S1) for 1 h at room temperature, protected from light. Samples were mounted and images were acquired as described above. Images were analyzed for nucleolar number and area via a custom CellProfiler 4.0 [17] pipeline.

DNA damage response marker foci analysis

Treated cells were induced, seeded, fixed, permeabilized, and blocked as above. Samples were incubated overnight at 4°C with gamma H2A.X, 53BP1, and lamin A/C primary antibodies (Table S1), followed by washes with 0.1% PBS-T. Appropriate secondary antibodies (Table S1) were incubated for 1 h at room temperature, followed by five washes with 0.1% PBS-T. Antibodies were diluted with 1% (v/v) bovine serum albumin (BSA, Millipore Sigma, A9418) in PBS. Samples were mounted using ProLong™ Diamond Antifade Mountant with DAPI. Image acquisition was performed using a Zeiss Observer Z1 microscope/ZEN pro 2.0 software (Carl Zeiss Microscopy). Images were analyzed via a custom CellProfiler 4.0 pipeline.

3D, confocal, live-cell imaging

Live cells were incubated for 45 min at standard conditions with 1 μg/mL of CellTracker™ Orange CMTMR (Invitrogen, #C2927) and 10 μM Vybrant™ DyeCycle™ Green Stain (Molecular Probes, # V35004) to label the cytoplasm and nucleus, respectively. Labeled cells were lifted and resuspended in cold Matrigel Basement Matrix (Corning, #356232), plated onto 35 mm Ibidi μ-Dishes (glass bottom, Ibidi USA Inc., #81158), and immediately coverslipped. Plated samples were cultured for 30 min at standard conditions to allow for solidification of the Matrigel, and then covered with phenol-free RPMI-1640 with L-Glutamine (Gibco, #1835030) with 10% FBS and 1% penicillin streptomycin. Image acquisition was performed using a Nikon Eclipse Ti2 microscope with a Nikon C2 camera and NIS Elements version 5.11. (Nikon Inc.) with a live-cell imaging ThermoBox incubation system (Tokai Hit Co.). 3D image processing and analysis was performed with Imaris 9.8 software (Oxford Instruments).

Time-lapse imaging of PC3-FUCCI

PC3-FUCCI cells were plated and cultured overnight under standard conditions (see above) and then treated with 6 μM cisplatin for 72 h. After treatment, media was changed and live-cell timelapse microscopy of treated cells was performed in an Incucyte SX5 (Sartorius). Images were taken every 30 min in the phase, green, and orange channels.

Flow cytometry analysis

Live cells were incubated with a FITC-Annexin V (BioLegend, #640906) according to the manufacturer's recommendations. Cells were analyzed on an Attune NxT Flow Cytometer (Thermo Fisher Scientific). At least 40,000 events were recorded per sample and acquired data was analyzed using FlowJo software version 10.8 (BD Biosciences).

Statistical analysis

All statistical analyses were performed in GraphPad Prism version 9.1 (GraphPad Software, LLC). An $\alpha = 0.05$ (confidence level 95%) was the criterion considered to determine statistical significance for all tests.

No significance (ns), *, **, ***, and **** represent p values of ≥0.05, <0.05, <0.01, <0.001, and <0.0001, respectively. For violin plots, red lines indicate median and blue lines indicate lower and upper quartiles.

Results

Cell death and survival after cisplatin treatment

Prostate cancer cell line PC3 was treated with 6 μM cisplatin for 72 h. Treatment effect, e.g., a LD 50, is typically evaluated immediately following therapy exposure, and we observed the expected cell die-off at 72 h. To characterize the cells that survive cisplatin treatment and then have the potential to go on to seed a resistant recurrence, we removed the chemotherapy and permitted the cultures to recover in complete media. Following release of cisplatin treatment, cells continued to die, though this cell death gradually decreased with time, and eventually plateaued (Fig. 1A, B). The number of surviving cells continues to decrease over time, with the highest level of cell death observed in the first three days post-cisplatin release (Fig. 1A, B). We evaluated apoptosis by flow cytometry for Annexin V stain. We found that the level of apoptosis was higher in the treated cultures compared to untreated control, but this difference decreased with increased recovery time out to three days post-treatment (Fig. 1C). Furthermore, we found that the surviving cells, after 10 days recovery from [LD50] cisplatin, are resistant to further therapies including docetaxel and etoposide (Fig. S1). To understand the cell biological phenotypes of cells that survive cisplatin treatment, we evaluated key morphological and functional features of surviving cells at various timepoints post-cisplatin treatment.

Increasing cellular and nuclear volume and repeated whole genome doubling in surviving cells over time

We assessed cell volume and nuclear volume of treated cells post treatment-release utilizing 3D confocal microscopy. The total cell volume of surviving cells increased over recovery time (Fig. 2A). Surviving cells also increased in nuclear volume over time (Fig. 2B). The nucleus-to-cytoplasm ratio gradually decreased as a function of recovery time (Fig. 2C). This implies that the rate of synthesis of non-nuclear biomolecules is relatively faster than genomic replication compared to treatment-naïve cells. To determine the extent to which the nuclear size was influenced by cytoskeletal/cytoplasmic components, we measured the area of isolated nuclei stained for lamin A/C (Fig. 2D, E). Consistent with the whole-cell data, the size of isolated nuclei increased with time from treatment (Fig. 2E).

The increasing nuclear size of the surviving cells suggested that mononucleated cells undergo repeated DNA duplication during the recovery period. We utilized a fluorescence ubiquitination cell cycle indicator (FUCCI) cell cycle sensor to track progression through cell cycle (Fig. 3A) [18]. The nuclei of cells transduced with the FUCCI construct fluoresce red in G1, yellow (double positive for red and green) in very early S, green in mid-late S, G2, and up to anaphase in M, and are colorless in late-M and G0 (Fig. 3B). Using live cell imaging, we observed large cisplatin-treated cells progressing through these different stages without undergoing cell division, a process termed endocycling (Fig. 2C). To specifically test for DNA replication, cultures were pulsed with thymidine analogue EdU. Positive EdU staining confirmed that mononucleated cells actively engaged in *de novo* DNA synthesis at all timepoints following removal of cisplatin (Fig. 3D). We additionally confirmed that the DNA content in the nuclei of the cells increased during the recovery period by measuring an integrated intensity of DAPI, which also increased over the recovery period (Fig. 3E). These findings indicate that surviving cells, while not proliferative, are functionally active in genome duplication.

Nuclear morphology of cells that survive cisplatin treatment

We classified the morphology of treated cancer cell nuclei as mononucleated or multinucleated. Conventional nuclear visualization by DNA staining with DAPI or Hoechst alone is not always suitable for distinguishing nucleus morphology (Fig. S2). The nuclear envelope of

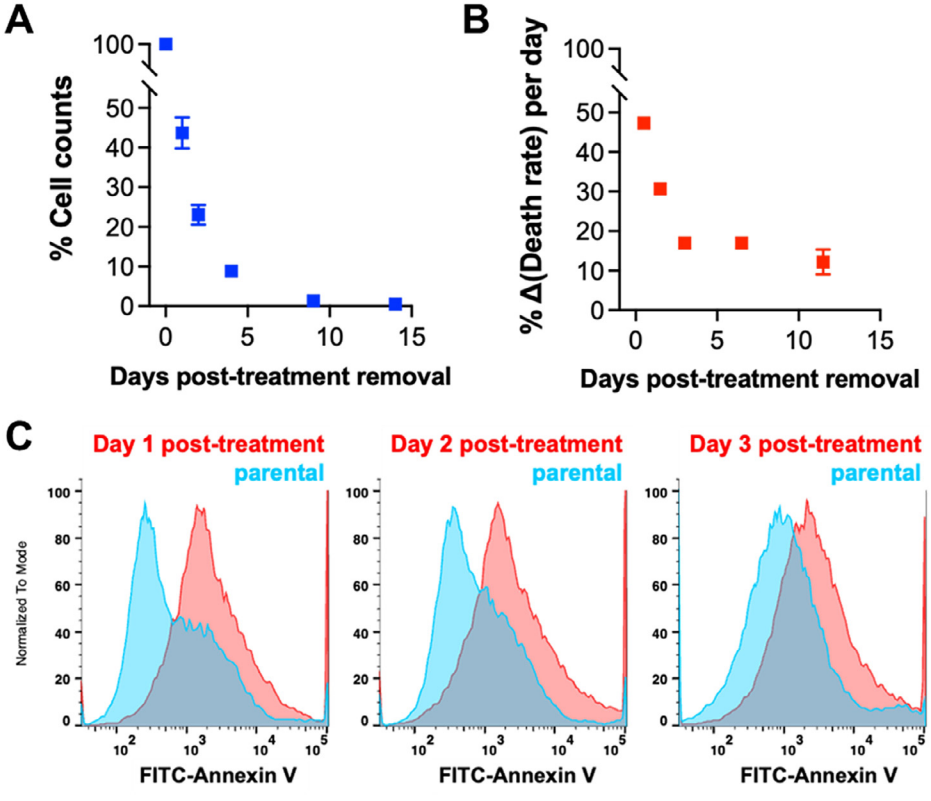

Fig. 1. Cell death and survival after cisplatin treatment. Relative cell number (percent normalized to population count at 0 days post-treatment removal) as a function of recovery time (A) was determined for treated PC3 cells generated with 72 h 6 μM [LD50] cisplatin treatment. From this data, we also determined (B) the percent change in the death rate for each of the recovery days we investigated. (C) Flow cytometry was used to measure surface expression of annexin V as a marker of apoptosis in treated PC3s generated with 72 h [LD50] cisplatin treatment at days 1, 2, and 3 post-treatment removal compared to parental PC3 prostate cancer cells.

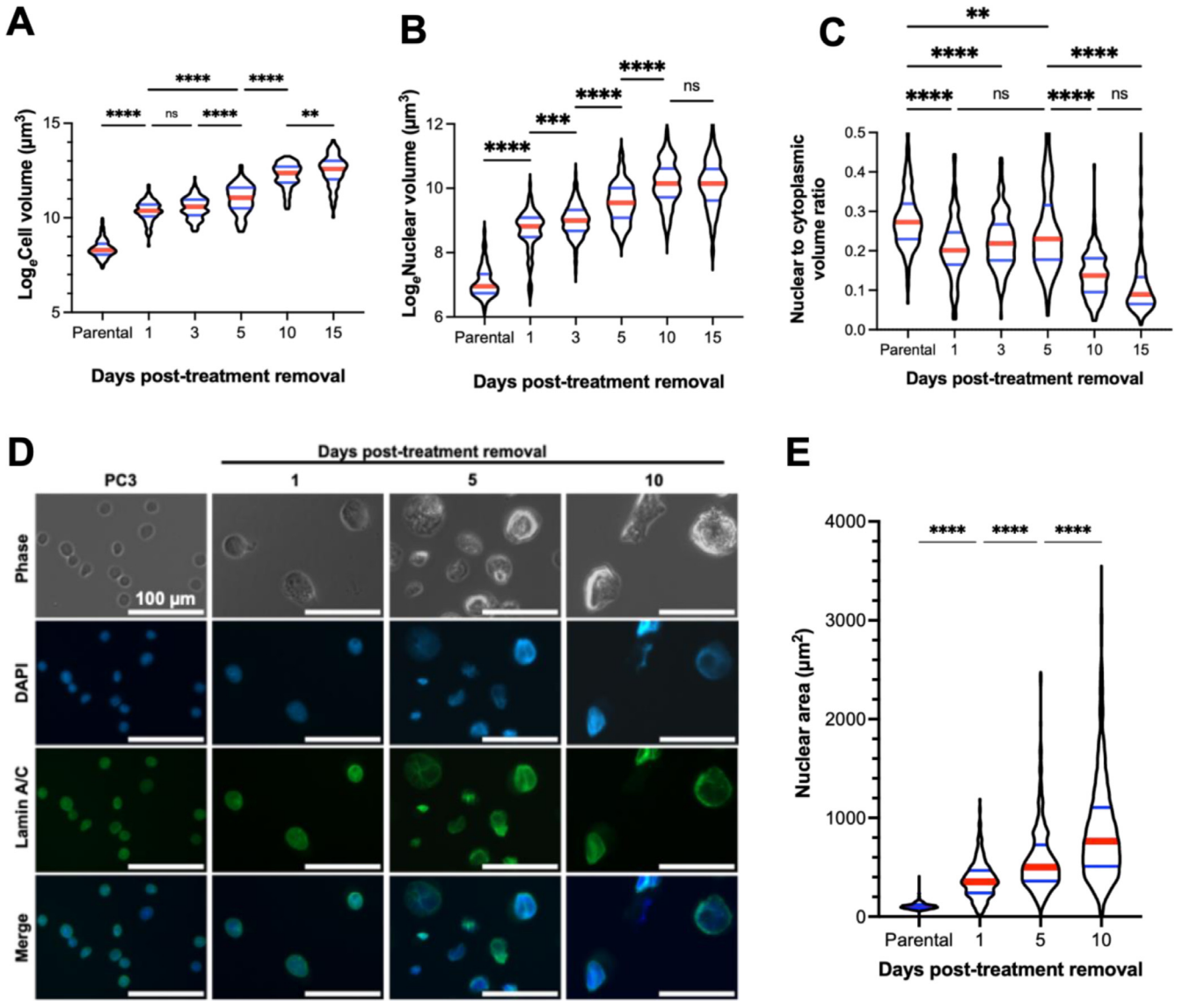

Fig. 2. Increasing cellular and nuclear volume in surviving cells over time. Natural log-transformed (A) cellular volume and (B) nuclear volume of live parental ($n = 214$) and treated PC3 cells, generated with 72h 6 µM cisplatin treatment, at various timepoints in recovery, day 1 ($n = 117$), day 3 ($n = 184$), day 5 ($n = 115$), day 10 ($n = 161$), and day 15 ($n = 120$), was determined by suspending cells in Matrigel and staining DNA with Vybrant™ DyeCycle™ Green Stain (for DNA) and CellTracker™ Orange (for cytoplasm). 3D images were obtained via confocal microscopy and images were rendered for volumetric determination using Imaris 9.8 software. Data was analyzed for differences between groups using a one-way ANOVA, a post-hoc Tukey's multiple comparisons tests was used to detect between-group differences. (C) Nuclear and cytoplasmic volumes were used to calculate a nuclear to cytoplasmic volume ratio of treated PC3s at various timepoints past treatment removal. A Kruskal-Wallis test was used to analyze if there were any significant differences among the samples, Dunn's multiple comparison's test used to test for comparisons between groups. (D) Nuclei were isolated from parental and treated PC3 cells before mounting on PLL-coated dishes. Nuclei were stained for lamin A/C and covered with ProLong™ Diamond Antifade Mountant with DAPI before imaging on a Zeiss Observer Z1 microscope. (E) The size of isolated nuclei of parental ($n = 825$) and treated PC3 cells, generated with 72h 6 µM cisplatin treatment, at various timepoints in recovery, day 1 ($n = 456$), day 5 ($n = 536$), day 10 ($n = 866$), was quantitated via a custom CellProfiler 4.0 pipeline. A Kruskal-Wallis test was used to analyze if there were any significant differences among the samples, Dunn's multiple comparison's test used to test for comparisons between groups. For all tests: $^{*} = p < 0.05$, $^{**} = p < 0.01$, $^{***} = p < 0.001$, $^{****} = p < 0.0001$.

cells was visualized by performing immunofluorescent labeling of lamin A/C to enhance visualization (Fig. 4A). To overcome limitations in 2D methodology due to a spatially hindering effect of the nuclear envelope signal (Fig. S3), we also utilized 3D confocal imaging (Fig. 4B). Immediately after removal from treatment, treated PC3 cells had a uniformly distributed nuclear morphology, with approximately equal proportion of mono- and multinucleates (Fig. 4C). As cells recovered, mononucleates became predominant over time by 2D imaging (Fig. 4C) and confirmed by 3D confocal microscopy imaging (Fig. 4D). Morphologically, the sphericity of nuclei gradually decreased over recovery time (Fig. 4G, H), suggesting that nuclei at later time points may exhibit high deformability, perhaps due to a lower supporting force derived from their cytoskeleton [5,19–21].

We tested cisplatin as a main chemotherapeutic in this study since it is a broadly used DNA-damaging agent. Thus, to evaluate the drug-specific phenotypic responses to treatment and recovery we evaluated surviving cells following treatment with the common chemotherapeutic drugs etoposide (topoisomerase II inhibitor) and docetaxel (microtubule stabilizer) for 72 h (Fig. 4E, F). The proportion of multinucleates was significantly different between the two drugs and compared to cisplatin. Increased proportion of multinucleated cells in the docetaxel treatment group are likely due to the mechanism of this therapy, which stabilizes

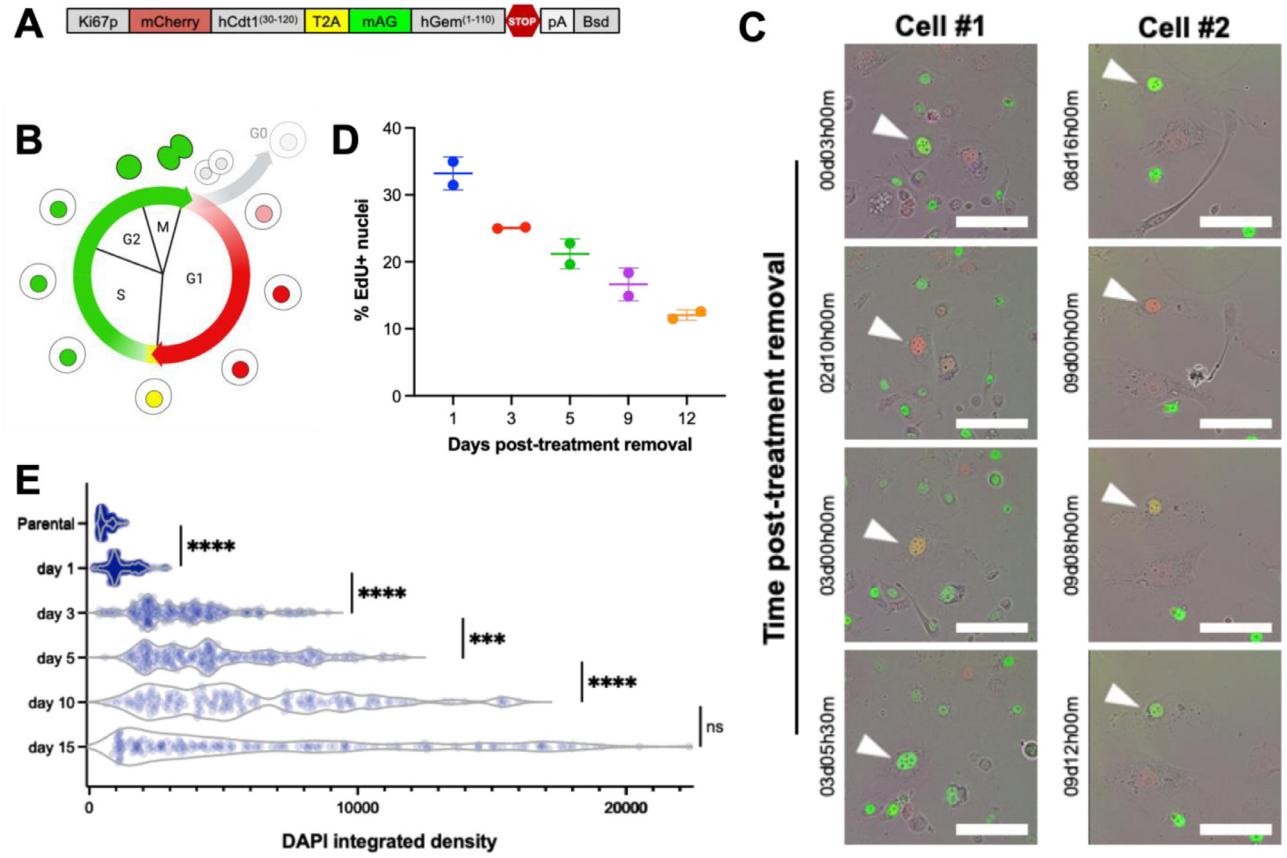

Fig. 3. Repeated whole genome doubling in the absence of cell division. PC3 cells were transduced with a (A) Ki67p-T2A-FUCCI construct, gifted from Alexander Zambon. (B, C) Treated PC3s were generated from this reporter cell line with 72 h 6 μM cisplatin treatment, and timelapse microscopy was performed with an Incucyte SX5 with images taken every 30 min after release from treatment, scale bar = 200 μm. Two representative cells are shown. (D) Cisplatin-treated PC3s were tested for *de novo* DNA synthesis via a Click-It Plus EdU assay according to the manufacturer's protocol. Images were acquired using the 10x objective on a Zeiss Observer Z1 microscope. A custom CellProfiler pipeline was developed and used to quantify DAPI+Edu+ nuclei. (E) PC3 cells were treated with 6 μM cisplatin for 72 h, and immunofluorescence imaging was used to visualize genomic contents as a measure of integrated DAPI intensity for parental PC3 cells (n = 529) and day 1 (n = 635), day 3 (n = 226), day 5 (n = 210), day 10 (n = 167), day 15 (n = 162) post-treatment removal. This was analyzed for differences between groups using a one-way ANOVA, a post-hoc Games-Howell's multiple comparisons tests was used to detect between-group differences. For these tests: *** = $p < 0.001$, **** = $p < 0.0001$.

microtubules, interrupting mitosis and inhibiting cell proliferation. Regardless of treatment type, all groups showed an increased proportion of mononucleated cells with recovery time. These results suggest that mononucleated PC3 cells will eventually become a dominant morphological phenotype in the longer recovery period.

DNA damage repair is retained in surviving cells

The DDR plays a crucial role in avoiding programmed cell death and prolonging cellular life [22]. gH2AX foci mark sites of DNA damage, and 53BP1 molecules form distinct foci when recruited to sites of DNA damage to initiate DNA repair [22]. To evaluate the extent of DNA damage and initiation of DDR, expression and colocalization of gH2AX and 53BP1 were assessed for each recovery time point (Fig. 5A, D).

Excessive DNA damage that induces acute apoptosis is distinguished by a pan-nuclear staining pattern of gH2AX [23,24]. The proportion of gH2AX pan-nuclear stained nuclei in treated cells was approximately 50% of the total population on day 1 and 30% on day 3 after cells were removed from treatment, gradually decreasing during recovery (Fig. 5E); this was consistent with our observations of overall cell death (Fig. 1A, B). We also evaluated gH2AX and 53BP1 foci per unit nuclei area in cells whose nuclei did not exhibit pan-nuclear stained gH2AX (Fig. 5B, C). In these experiments, we observed that the total number of gH2AX foci generally increased early in the period of recovery from treatment, and later decreased to parental levels at days 10 and 15 post-treatment removal. The number of 53BP1 foci decreased until day 3 and then returned to pre-treatment levels by the later recovery timepoints (Fig. 5C). Colocalization of gH2AX and 53BP1 foci are indicative of intact DNA damage repair. Early in recovery (days 1 and 3), treated cells had a low level of colocalization, but the colocalized gH2AX/53BP1 foci returned to the level of the untreated cancer cell control at day 10 post-treatment (Fig. 5D). Over time, the size of gH2AX foci decreased, whereas the size of 53BP1 foci increased following therapy from day 1 to day 10 (Fig. S4). Together, these findings suggest that surviving cells activate the DDR pathway to avoid cell death [22].

We found that mononucleate cells became the dominant population over the duration of treated cell recovery (Fig. 4C-D), suggesting that multinucleated cancer cells died. To investigate the activation of the DDR in these distinct nuclear morphologies, the level of colocalization between gH2AX and 53BP1 foci in each type was compared (Figs. 5F, S5). Mononucleate cells contain more colocalized DDR foci than multinucleates, suggesting that mononucleated cells retained intact DNA damage of repair that was not observed in multinucleated cells. A primary mechanism of multinucleate formation is a mitotic catastrophe [6,9,13]. The proportion of nuclei that underwent a mitotic catastrophe in cisplatin treated PC3 was determined by examining immunofluorescent-labeled images of the nuclear envelope (Fig. 5G, H). The results indicate that proportion of mitotic catastrophe in treated PC3 cells decreased in the recovery period. These findings suggest that an active DDR may

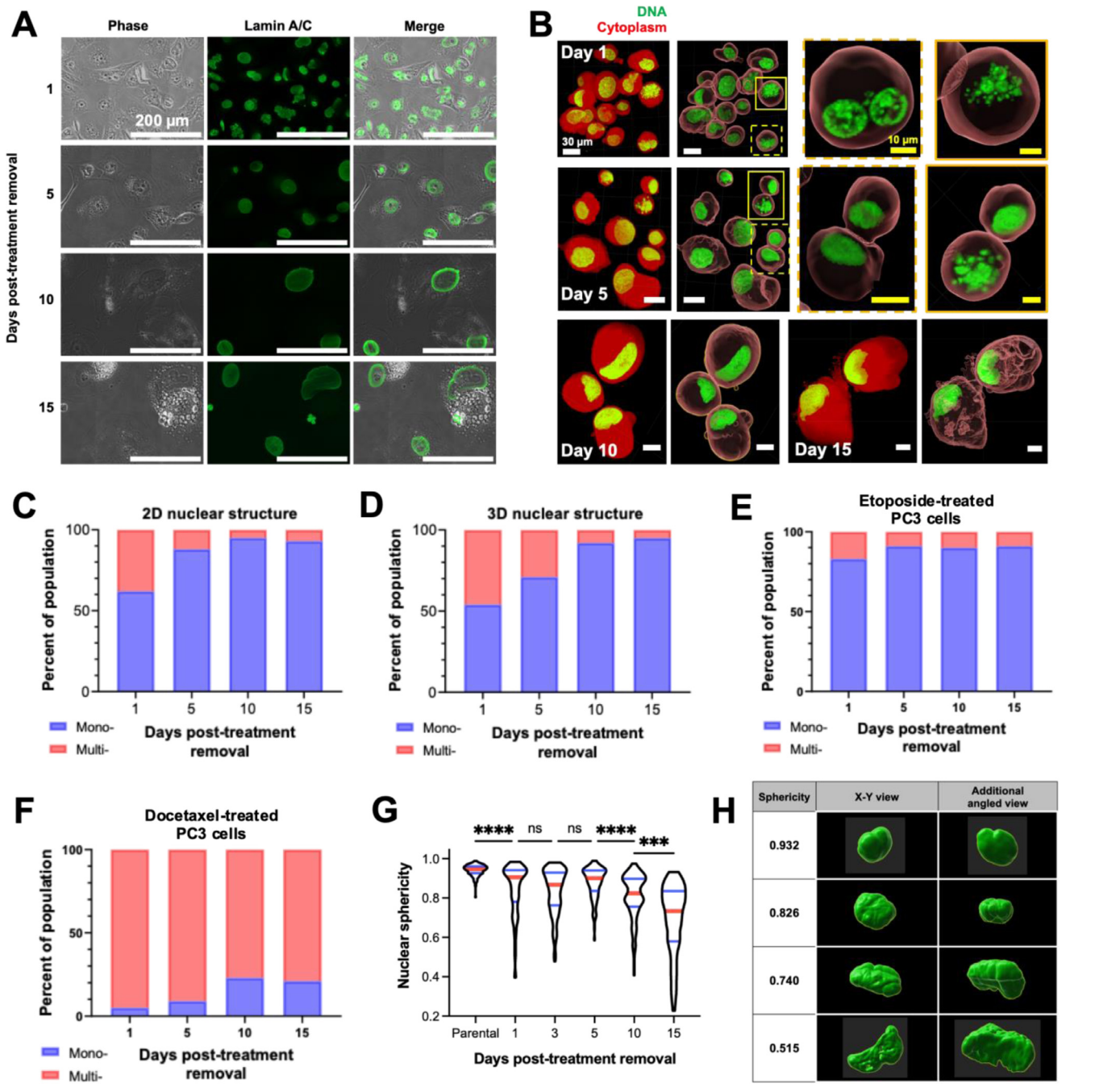

Fig. 4. Characterization of the nuclear morphology of cisplatin-treated prostate cancer cells. Representative immunofluorescence images (A) to demonstrate the nuclear morphology of treated PC3 cells generated with 72 h 6 μM cisplatin treatment following removal from chemotherapy. (B) Live treated PC3 cells at various timepoints in recovery were suspended in Matrigel and staining DNA with Vybrant™ DyeCycle™ Green Stain (for DNA) and CellTracker™ Orange (for cytoplasm). 3D images were obtained via confocal microscopy and images were rendered and volumes determined using Imaris 9.8 software. (C) Population distribution of mononucleated and multinucleated PC3s, derived from images described in (A). Nuclear morphology (mononucleated vs. multinucleated) was manually discriminated and counted using Fiji. At least 250 cells were analyzed per condition. (D) Nuclear morphology was also determined using the 3D images described in (B). The population distribution of mononucleated and multinucleated treated PC3 cells generated with 72h (E) 25 μM etoposide treatment or (F) 5 nM docetaxel treatment was also determined, derived from immunofluorescent images of cells stained for lamin A/C and mounted with DAPI. Nuclear morphology (mononucleated vs. multinucleated) was discriminated and counted in Fiji software.

contribute to avoiding multinucleation due to mitotic catastrophe that prevents cell death.

Nucleolar size increases and number decreases following cisplatin treatment release

The primary substructure of the nucleus is the nucleolus, an rRNA production hub that plays a significant role in nuclear homeostasis [25,26]. We found that the number of nucleoli within the nuclei of treated PC3 cells decreased (Fig. 6A, B), while the average size of each nucleolus increased (Fig. 6A, C) over recovery time. The nucleolar to nuclear area ratio in treated cells initially decreased at early time points (until day 3) and rebounded during recovery (Fig. 6D). These results indicate that the synthesis of nucleolar molecules was initially slower than nuclear molecules in treated cells; however, this area ratio returns to relative levels similar to untreated con-

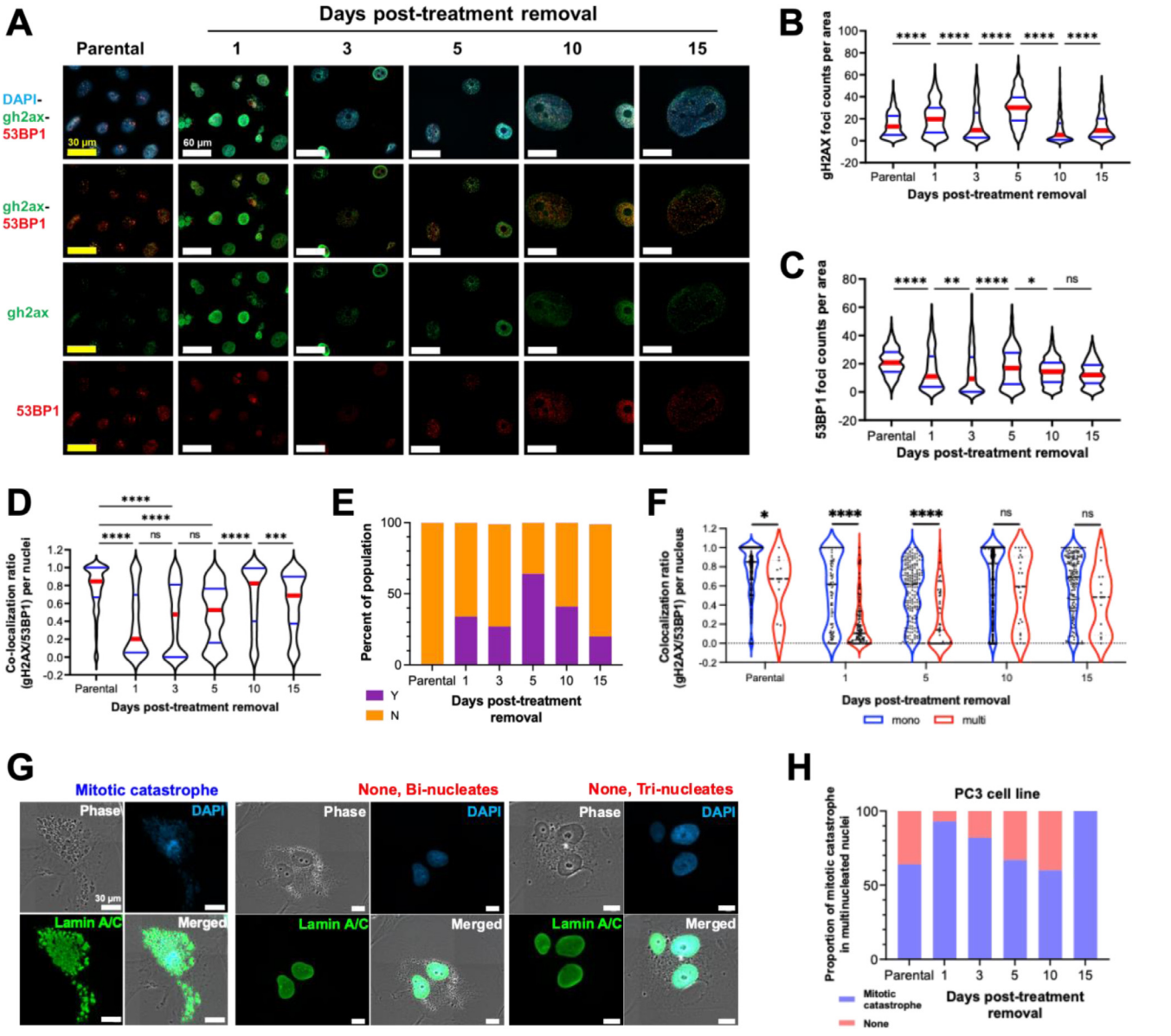

Fig. 5. The DNA damage response in cisplatin-treated prostate cancer cells. PC3 cells were treated with 6 µM cisplatin for 72h. (A) Immunofluorescence staining and imaging was used to visualize genomic contents (DAPI), sites of DNA damage (gH2AX), and DDR machinery recruitment (53BP1). From these images, a custom CellProfiler 4.0 pipeline was used to determine raw count per unit cellular area of the number of (B) gH2AX foci and (C) 53BP1 foci, as well as (D) the colocalization ratio of gH2AX with 53BP1. (E) The relative proportion of cells with (Y) and without (N) gH2AX pan-nuclear stained nuclei from was determined. (F) For each day post-treatment recovery, cells were classified as mononucleates and multinucleates, and the colocalization ratio of gH2AX with 53BP1 was determined for each cell class. Mononucleated, multinucleated, and mitotically catastrophic cells were classified via a custom CellProfiler 4.0 pipeline, and (G-H) the proportion of multinucleated cells to those experiencing mitotic catastrophe were plotted across the different days post-treatment removal. Mann-Whitney tests were used to detect differences between groups in (B), (C), (D), and (F). For all tests: $^{*} = p < 0.05$, $^{**} = p < 0.01$, $^{***} = p < 0.001$, $^{****} = p < 0.0001$.

trols, suggesting the potential of nucleoli to actively respond to genomic stress during treatment recovery to maintain nuclear homeostasis [26,27].

In its function as a ribosomal RNA production hub, a nucleolus contains genes for rRNAs [25,26]. We found that the level of 28S rRNA in treated PC3 cells was higher than that in non-treated cells and that it increased with recovery time. 18S rRNA expression was lower in treated cells overall, while the level of 5.8S rRNA remained similar in all conditions (Fig. S6). The altered rRNA composition of cells recovering from cisplatin treatment suggests that the remodeling of rRNA configuration in the nucleolus may be a response to genomic stress.

Discussion and conclusions

The majority of studies that describe lethal or inhibitory concentrations of therapies look at a single time point, e.g., how many cells die at 72 h. Furthermore, most of the assays used to assess therapeutic effect do not look at the morphology of cells at the time of assay. In this study, we explored the life history of cells in the days and weeks after cisplatin treatment to gain insights into the adaptive characteristics of surviving cells that are likely to seed eventual recurrence. We found that cells that resist therapy-induced cell death are predominantly mononucleated and undergo multiple rounds of genome duplication without cell division in a process of endocycling, resulting in increased nuclear size and

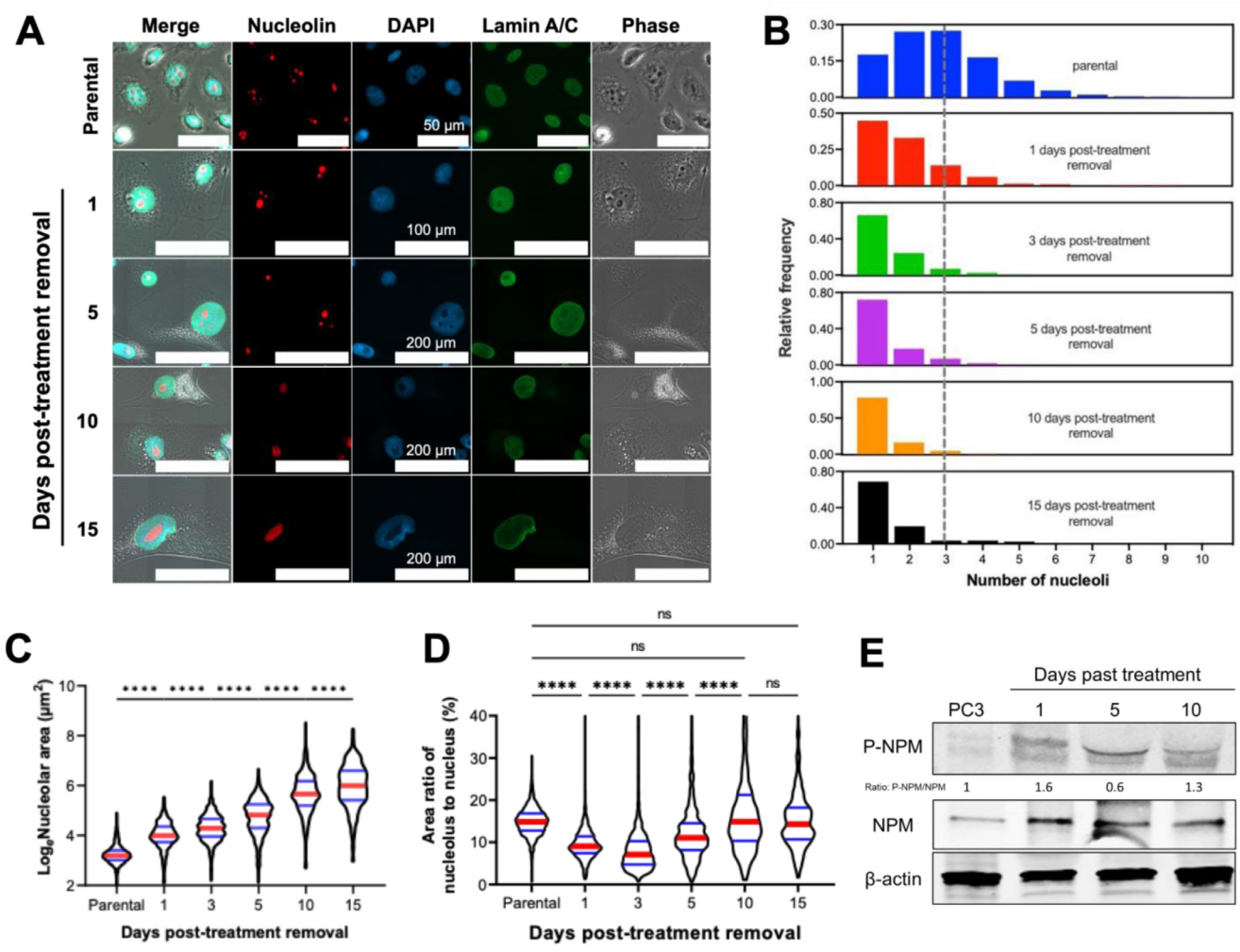

Fig. 6. Nucleolar counts, size, and molecular signatures. Treated PC3 cancer cells generated with 72h 6 μM cisplatin treatment were stained for lamin A/C and nucleolin, and were mounted with DAPI, (A) representative images of nucleoli are shown. A custom CellProfiler 4.0 pipeline was used to then determine the (B) number and (C) area of the nucleoli of the treated PC3s throughout the recovery period to post-treatment removal. Nucleolar area was analyzed for differences between groups using a one-way ANOVA, and a post-hoc Tukey's multiple comparisons test was used to detect between-group differences. The lamin A/C stain was used to calculate nuclear area, and thus (D) the nucleolar to nuclear area ratio at each timepoint post-treatment removal could be calculated (E) Expression of phosphorylated nucleophosmin (P-NPM) and total nucleophosmin (NPM) in PC3 cells and PC3s post-treatment removal; a Kruskal-Wallis test was used to analyze if there were any significant differences among the samples, with a Dunn's multiple comparison's post-hoc test. For all statistical tests: $^{*} = p < 0.05$, $^{**} = p < 0.01$, $^{***} = p < 0.001$, $^{****} = p < 0.0001$.

increased cell size. We further find that cells that survive after therapy release retain continued DDR and contain active nucleoli that produce increased rRNA levels. These findings represent a new understanding of at least one way cancer cells resist cytotoxic therapy and contribute to cancer lethality.

We observed dramatic increases in the nuclear volume of cells post-treatment removal over time (Fig. 2), representing a 70-fold increase over untreated cells at the latest timepoint measured. Combined with evidence of continued S-phase DNA synthesis in cells that survived after cisplatin treatment, this suggests that surviving cancer cells have undergone multiple whole genome doublings, or polyploidization events. It is generally accepted in the field that polyploid cells that form after chemotherapeutic treatment are multinucleated [4,10,11,28]. We found, however, that not only do mononucleated cells exist, but that a mononucleate morphology is the predominant cell type over the course of cellular recovery from cisplatin, docetaxel, and etoposide therapy in PC3 cells. Nuclear morphology (i.e., mononuclear vs multinuclear) provides valuable insight regarding mechanisms of therapeutic survival. We show that the surviving cells engage in active DNA replication without entry into mitosis (Fig. 3), a process known as endocycling, providing a mechanistic explanation for the increase in nuclear size that we observed and that others have observed in studies of similarly large, polyploid cancer cells [4,6,10,11,28]. Meanwhile, cytoplasmic volumes steadily increased over time, suggesting consistent biosynthesis of other non-genomic cellular contents. With increasing nuclear volume, we further show that treated cells had decreasing nuclear sphericity as a function of recovery time. Nuclear circularity, and its 3D counterpart sphericity, is a representative feature of morphological abnormalities [29,30]. Nuclear deformability is critical for successful invasion and migration during the metastatic process [5,19], and decreased sphericity implies capacity for deformability. The decreased sphericity of surviving cells is consistent with previous reports that large, polyploid cancer cells may have increased metastatic potential [31,32].

To investigate the cellular response to treatment-induced DNA damage in treated cells that eventually die versus those that survive following release from treatment, we simultaneously evaluated DNA damage via gH2AX staining and initiation of DNA damage repair via recruitment of 53BP1. As expected, we initially observed a high level of catastrophic and widespread DNA damage (including increased gH2AX foci counts and gH2AX pan-nuclear staining) that decreased as cell populations

recovered (Fig. 5A, B), consistent with the observed high levels of apoptosis at early timepoints (Fig. 1C). Conversely, colocalization of gH2AX and 53BP1 foci as a surrogate for initiation of DDR increased over recovery time and colocalization was increased in mononucleated versus multinucleated cells at every time point (Fig. 5D, F). Simultaneously, the relative death rate of treated cells decreased with time (Fig. 1B), suggesting that intact DDR in mononucleated cells is associated with survival. Notably, 53BP1 nuclear pan-nuclear staining, recognized as a failure of its recruitment to DNA damage sites [24,33,34], was not observed at any timepoint, suggesting that DDR was intact in the surviving cell populations.

Together, these data support a paradigm where soon after therapy release, the treated population contains a higher proportion of cells with a high level of widespread and catastrophic DNA damage that leads to apoptosis, while those cells that have successful DDR are more likely to access a pro-survival state. Within the polyploid cell populations that initially survive therapeutic insult, we find that multinucleated cells often exhibit high rates of mitotic catastrophe, even at later timepoints following therapy release (Fig. 5G, H). Over recovery time, we observed fewer multinucleated cells in the surviving population, simultaneous with a lower rate of cell death (Fig. 4), further indicating that mononucleated cells are more successful at survival once the chemotherapeutic treatment is released. The presence of additional genomic material inside an enlarged, mononucleated cancer cell may reinforce the genetic stability of these cells and enhance their resiliency against varied environmental stressors.

The nucleolus plays a crucial role in nuclear homeostasis as an RNA production hub [25,26]. We demonstrate that cells that survive long after cisplatin treatment contained fewer nucleoli of a larger size with a corresponding increased rRNA production (Fig. 6B, C; Fig. S6). This distinct pattern may be a consequence of endocycling since in normally dividing cells the nucleolar structure disassembles at the mitotic phase and reassembles at interphase [25]. Smaller but more numerous nucleoli are highly correlated with cancer malignancy and have previously been used as a diagnostic signature [27], while our data suggest that fewer, larger nucleoli can also be indicative of cancer cells that persist despite chemotherapeutic insult. Interestingly, stem cells, however, have been reported to have a similar nucleolar signature as surviving cells: fewer but larger nucleoli than differentiated somatic cells [35]. Other studies of large, polyploid cancer cells have suggested that they may act as a type of cancer stem cell, possessing stem cell-like features and cellular programs [4,6,8,9,11,15], highlighting the potential of exploring these surviving cells as critical recurrence-mediating cells.

These observations support an underappreciated conserved mechanism of cancer cell survival following stresses such as anti-cancer therapy that has been reported in the literature as the polyaneuploid cancer cell (PACC) state, polyploid giant cancer cells (PGCCs), pleomorphic giant cancer cells, osteoclast-like cells, and persister cells, among other names. The PACC state is initiated when a cancer cell is subjected to a stressor, such as chemotherapy or radiotherapy, triggering a conserved evolutionary program that results in sustained polyploidization of the aneuploid genome (polyaneuploidy) and increased cell size and cell contents. When the cellular stressor is no longer present, and after a period of recovery, cells exit the PACC state and reinitiate mitotic proliferation, a phenomenon clinically observed as cancer recurrence. Recent pieces of evidence show the PACC state is a functional response more than a stochastic escape from stressors [4,9–12]. Cells in the PACC state have been identified in the tumors of patients with various cancer types including prostate, ovarian, and breast [36–38], and presence of cells in the PACC state in clinical radical prostatectomy specimens from prostate cancer patients is predictive of an increased risk of disease recurrence [39]. The fundamental characteristics of the PACC state, however, including nuclear morphology (critical for understanding DNA packaging of a multi-polyploid cell) and mechanism of entry and maintenance in this PACC state, are unclear.

Growing investigation into the role of the PACC states relevant to cancer lethality suggests that the PACC state is a “hallmark of lethal cancer” [9]. The findings presented in this study suggest that mononucleated cells in the PACC state are critical players in therapy survival and to eventual cancer recurrence. These data indicate at least two distinct fates of cancer cells following treatment: (1) cells with catastrophic, irreparable DNA damage undergo apoptosis or other forms of cell death; and (2) cells engage DDR survive and engage in continued endocycling, leading to a predominantly mononuclear cell population with increased nuclear size and nucleolar size and capacity. We showed that mononuclear cells in the PACC state had higher evidence of DDR and increased survival, indicating mononucleation, or the processes that lead to that nuclear morphology, offers a survival advantage over multinucleation. Conversely, cells with a multinucleate morphology have apparently lower levels of DDR, higher rates of mitotic catastrophe, and lower survival over time. Given the increased nuclear size and endocycling observed in mononucleated cells in the PACC state, it is likely that these multinucleated cells eventually activate the cell-cycle checkpoints that they initially bypass to enter a polyploid state, thus triggering apoptosis. While this is a key observation, further work is needed to elucidate if this multinucleation is the cause or consequence of such cell cycle checkpoint activation. The characterization of structural morphological characteristics of the resistant cells in the PACC state highlight a number of compelling routes for future study, including the structural phenotypes that are associated with and / or enable survival of malignant cells. Additional studies are needed to understand the unique and shared characteristics and plasticity of the cells in the PACC state with other cell states that share these structural characteristics, e.g., senescent cells and stem cells. Further characterization of the cellular and molecular programs that cancer cells in this state can be leveraged to understand phenotypes that contribute to cancer lethality.

Data availability statement

Data were generated by the authors and available on request from the corresponding authors.

Financial support

This work was supported by the Basic Science Research Program through the National Research Foundation of Korea, funded by the Ministry of Education [grant number 2021R1A6A3A14043146]; the Institute for Basic Science, Republic of Korea [grant number IBS-R020-D1]; the National Cancer Institute grants [grant numbers U54CA143803, CA163124, CA093900, and CA143055]; the US Department of Defense Congressionally Directed Medical Research Programs/Prostate Cancer Research Program [grant numbers W81XWH-20-10353 and W81XWH-22-1-0680]; the Prostate Cancer Foundation; and the Patrick C. Walsh Prostate Cancer Research Fund.

Declaration of Competing Interest

Kenneth J Pienta is a consultant for CUE Biopharma, Inc., and holds equity interest in CUE Biopharma, Inc., Keystone Biopharma, Inc. and PEEL Therapeutics, Inc. Sarah R Amend holds equity interest in Keystone Biopharma, Inc.

CRediT authorship contribution statement

Chi-Ju Kim: Conceptualization, Methodology, Investigation, Writing – original draft, Writing – review & editing, Visualization. **Anna LK Gonye:** Conceptualization, Methodology, Investigation, Writing – original draft, Writing – review & editing, Visualization. **Kevin Truskowski:** Methodology, Investigation. **Cheng-Fan Lee:** Investigation. **Yoon-Kyoung Cho:** Conceptualization, Writing – review & editing, Funding acquisition. **Robert H. Austin:** Conceptualization, Writing – review & editing. **Kenneth J. Pienta:** Conceptualization, Writing

– review & editing, Funding acquisition. **Sarah R. Amend:** Conceptualization, Writing – review & editing, Funding acquisition.

Acknowledgments

The authors thank members of the Cancer Ecology Center for thoughtful discussion and feedback.

Supplementary materials

Supplementary material associated with this article can be found, in the online version, at doi:10.1016/j.neo.2023.100906.

References

[1] EG Fischer, Nuclear morphology and the biology of cancer cells, Acta Cytol. 64 (2020) 511–519.
[2] LF Flores, BR Tader, EJ Tolosa, AN Sigafoos, DL Marks, ME Fernandez-Zapico, Nuclear Dynamics and chromatin structure: implications for pancreatic cancer, Cells 10 (2021) 2624.
[3] C Koch, A Kuske, SA Joosse, G Yigit, G Sflomos, S Thaler, DJ Smit, S Werner, K Borgmann, S Gärtner, et al., Characterization of circulating breast cancer cells with tumorigenic and metastatic capacity, EMBO Mol. Med. 12 (2020).
[4] R Mirzayans, B Andrais, D Murray, Roles of Polyploid/multinucleated giant cancer cells in metastasis and disease relapse following anticancer treatment, Cancers 10 (2018) 118.
[5] C Denais, J Lammerding, in: Nuclear Mechanics in Cancer, Springer, New York, 2014, pp. 435–470.
[6] SR Amend, G Torga, KC Lin, LG Kostecka, A Marzo, RH Austin, KJ Pienta, Polyploid giant cancer cells: Unrecognized actuators of tumorigenesis, metastasis, and resistance, Prostate 79 (2019) 1489–1497.
[7] LG Kostecka, KJ Pienta, SR Amend, Lipid droplet evolution gives insight into polyaneuploid cancer cell lipid droplet functions, Med. Oncol. 38 (2021).
[8] KJ Pienta, EU Hammarlund, RH Austin, R Axelrod, JS Brown, SR Amend, Cancer cells employ an evolutionarily conserved polyploidization program to resist therapy, Semin. Cancer Biol. (2020).
[9] KJ Pienta, EU Hammarlund, JS Brown, SR Amend, RM Axelrod, Cancer recurrence and lethality are enabled by enhanced survival and reversible cell cycle arrest of polyaneuploid cells, Proc. Natl Acad. Sci. 118 (2021) e2020838118.
[10] T Illidge, Polyploid giant cells provide a survival mechanism for p53 mutant cells after DNA damage, Cell Biol. Int. 24 (2000) 621–633.
[11] J Chen, N Niu, J Zhang, L Qi, W Shen, VK Donkena, Z Feng, J Liu, Polyploid giant cancer cells (PGCCs): the evil roots of cancer, Curr. Cancer Drug Targets 19 (2019) 360–367.
[12] K-C Lin, G Torga, Y Sun, R Axelrod, KJ Pienta, JC Sturm, RH Austin, The role of heterogeneous environment and docetaxel gradient in the emergence of polyploid, mesenchymal and resistant prostate cancer cells, Clin. Exp. Metastasis 36 (2019) 97–108.
[13] KJ Pienta, EU Hammarlund, R Axelrod, JS Brown, SR Amend, Poly-aneuploid cancer cells promote evolvability, generating lethal cancer, Evol. Appl. 13 (2020) 1626–1634.
[14] K-C Lin, Y Sun, G Torga, P Sherpa, Y Zhao, J Qu, SR Amend, KJ Pienta, JC Sturm, RH Austin, An *in vitro* tumor swamp model of heterogeneous cellular and chemotherapeutic landscapes, Lab Chip 20 (2020) 2453–2464.
[15] MM Mallin, KJ Pienta, SR Amend, Cancer cell foraging to explain bone-specific metastatic progression, Bone (2020) 115788.
[16] J Schindelin, I Arganda-Carreras, E Frise, V Kaynig, M Longair, T Pietzsch, S Preibisch, C Rueden, S Saalfeld, B Schmid, et al., Fiji: an open-source platform for biological-image analysis, Nat. Methods 9 (2012) 676–682.
[17] DR Stirling, MJ Swain-Bowden, AM Lucas, AE Carpenter, BA Cimini, A Goodman, CellProfiler 4: improvements in speed, utility and usability, BMC Bioinform. 22 (2021) 433.
[18] AC Zambon, T Hsu, SE Kim, M Klinck, J Stowe, LM Henderson, D Singer, L Patam, C Lim, AD McCulloch, et al., Methods and sensors for functional genomic studies of cell-cycle transitions in single cells, Physiol. Genom. 52 (2020) 468–477.
[19] T Fischer, A Hayn, CT Mierke, Effect of nuclear stiffness on cell mechanics and migration of human breast cancer cells, Front. Cell Dev. Biol. 8 (2020).
[20] GR Kidiyoor, Q Li, G Bastianello, C Bruhn, I Giovannetti, A Mohamood, GV Beznoussenko, A Mironov, M Raab, M Piel, et al., ATR is essential for preservation of cell mechanics and nuclear integrity during interstitial migration, Nat. Commun. 11 (2020).
[21] T Takaki, M Montagner, MP Serres, M Le Berre, M Russell, L Collinson, K Szuhai, M Howell, SJ Boulton, E Sahai, et al., Actomyosin drives cancer cell nuclear dysmorphia and threatens genome stability, Nat. Commun. 8 (2017) 16013.
[22] S Panier, SJ Boulton, Double-strand break repair: 53BP1 comes into focus, Nat. Rev. Mol. Cell Biol. 15 (2014) 7–18.
[23] B Meyer, K-O Voss, F Tobias, B Jakob, M Durante, G Taucher-Scholz, Clustered DNA damage induces pan-nuclear H2AX phosphorylation mediated by ATM and DNA–PK, Nucleic Acids Res. 41 (2013) 6109–6118.
[24] Feraudy Sd, I Revet, V Bezrookove, L Feeney, JE Cleaver, A minority of foci or pan-nuclear apoptotic staining of γH2AX in the S phase after UV damage contain DNA double-strand breaks, Proc. Natl Acad. Sci. 107 (2010) 6870–6875.
[25] D Hernandez-Verdun, Assembly and disassembly of the nucleolus during the cell cycle, Nucleus 2 (2011) 189–194.
[26] L Latonen, Phase-to-phase with nucleoli – stress responses, protein aggregation and novel roles of RNA, Front. Cell. Neurosci. 13 (2019).
[27] I Orsolic, D Jurada, N Pullen, M Oren, AG Eliopoulos, S Volarevic, The relationship between the nucleolus and cancer: current evidence and emerging paradigms, Semin. Cancer Biol. 37-38 (2016) 36–50.
[28] Z Zhang, X Feng, Z Deng, J Cheng, Y Wang, M Zhao, Y Zhao, S He, Q Huang, Irradiation-induced polyploid giant cancer cells are involved in tumor cell repopulation via neosis, Mol. Oncol. (2021).
[29] AFJ Janssen, SY Breusegem, D Larrieu, Current methods and pipelines for image-based quantitation of nuclear shape and nuclear envelope abnormalities, Cells 11 (2022) 347.
[30] M Schöchlin, SE Weissinger, AR Brandes, M Herrmann, P Möller, JK Lennerz, A nuclear circularity-based classifier for diagnostic distinction of desmoplastic from spindle cell melanoma in digitized histological images, J. Pathol. Inform. 5 (2014) 40 -40.
[31] MM Mallin, N Kim, MI Choudhury, SJ Lee, SS An, SX Sun, K Konstantopoulos, KJ Pienta, SR Amend. Cells in the polyaneuploid cancer cell (PACC) state have increased metastatic potential, *Biorxiv*. (2022) doi:10.1101/2022.09.16.508155.
[32] B Xuan, D Ghosh, MR Dawson, Contributions of the distinct biophysical phenotype of polyploidal giant cancer cells to cancer progression, Semin. Cancer Biol. 81 (2022) 64–72.
[33] E Bártová, S Legartová, M Dundr, J Suchánková, A role of the 53BP1 protein in genome protection: structural and functional characteristics of 53BP1-dependent DNA repair, Aging 11 (2019) 2488–2511.
[34] M Zimmermann, T De Lange, 53BP1: pro choice in DNA repair, Trends Cell Biol. 24 (2014) 108–117.
[35] S Gupta, R Santoro, Regulation and roles of the nucleolus in embryonic stem cells: from ribosome biogenesis to genome organization, Stem Cell Rep. 15 (2020) 1206–1219.
[36] R Mannan, X Wang, PS Bawa, DE Spratt, A Wilson, J Jentzen, AM Chinnaiyan, ZR Reichert, R Mehra, Polypoidal giant cancer cells in metastatic castration-resistant prostate cancer: observations from the Michigan Legacy Tissue Program, Med. Oncol. 37 (2020) 16.
[37] JS Richards, NR Candelaria, RB Lanz, Polyploid giant cancer cells and ovarian cancer: new insights into mitotic regulators and polyploidydagger, Biol. Reprod. 105 (2021) 305–316.
[38] G Saini, S Joshi, C Garlapati, H Li, J Kong, J Krishnamurthy, MD Reid, R Aneja, Polyploid giant cancer cell characterization: new frontiers in predicting response to chemotherapy in breast cancer, Semin. Cancer Biol. 81 (2022) 220–231.
[39] AM Alharbi, AM De Marzo, JL Hicks, TL Lotan, JI Epstein, Prostatic adenocarcinoma with focal pleomorphic giant cell features a series of 30 cases, Am. J. Surg. Pathol. 42 (2018) 1286–1296.